TRANSPORT OF SOLIDS IN A SCREW FEEDER

by

CHERNG-CHIAO WU

B.S., National Taiwan University, 1973

A MASTER'S THESIS

submitted in partial fulfillment of the

requirements for the degree

MASTER OF SCIENCE

Department of Chemical Engineering

KANSAS STATE UNIVERSITY

Manhattan, Kansas

1978

Approved by:

Walter P. Walawender

Major Professor

Document
LD
2668
.T4
1978
W91
C.2

ACKNOWLEDGMENTS

The author wishes to express his sincere appreciation to Dr. W. P. Walawender, for his constant advice and guidance during the course of this research and the writing of this thesis.

The author also wishes to express his gratitude to Dr. L. T. Fan for his experienced advice; to Dr. J. C. Matthews for serving as the supervisory committee member; to the secretaries of the Chemical Engineering Department of Kansas State University, for their extreme care in typing of the manuscript; to Kansas State Agriculture Experiment Station for their financial support (Grant No. 0946).

The author also wishes to express his sincerest to his parents, Mr. and Mrs. Song - Pei Wu, and to his friend Ming, their continuous encouragement made possible the completion of this work.

TABLE OF CONTENTS

LIST OF ILLUSTRATIONS

LIST OF TABLES

CHAPTER 1

INTRODUCTION

The screw feeder has been widely used as a feeding device for granular solids. The salient feature of the screw transport process is an Achimedian screw rotating in a cylindrical barrel. This method has the advantages of compactness, simplicity, stability, economics and consequently its use is desirable in many situations. But it is in the field of solids handling that screws have their greatest application. Typical uses are as a screw conveyor or a screw elevator in agriculture for moving grain, feed, and other granular materials, as screw feeder for measuring or feeding fragmented materials in industry, and as extruder to transfer materials against elevated pressure in the polymer industry. The scale of equipment varies from small single units to large sequential installations. A less common application is in large-scale pumping of fluids such as in irrigation.

The classification of screw equipment types is usually based on their functions, e.g.: conveyor, elevator, feeder, extruder. The conveyor is designed to transport materials. The screw rotates in either a barrel or a U shape trough. Generally a screw conveyor operates at less than its maximum capacity and consequently the screw is only partially full. The screw elevator is an inclined screw conveyor, and is used to lift materials.

The screw feeder is designed to provide a controlled feed of bulk material. In this application, the screw is enclosed in a cylindrical barrel. In this case the material generally fills the entire chamber. Regulation of the feed rate is achieved by adjusting the rotational speed of the screw. The extruder has the same features as the screw feeder, but, in addition, it has the ability to withstand high back pressure and high temperature.

The demarcation between these classes is vague, since the same equipment is often designed to perform two or more of the functions; a conveyor can be used to regulate feed rate, or as a feeder. A feeder can be used to transport material or as a conveyor.

Because of the complex dynamic behavior of the granular material in passing through a screw, an accurate account of the true conveying action is very difficult. Attempts have been made to analyze the screw conveying mechanism using somewhat simplified concepts by agricultural engineers. With the growth of the polymer industry, extruders have been the subject of extensive studies on the transport of polymer melt in the extruder. However, the solids conveying zone has been the subject of much less attention than the melt zone. Some theories have been proposed to estimate the delivery rate of the screw conveying device, but at present, the existing treatment is inadequate.

The object of this study is to formulate a theoretical approach for estimating the delivery rate of a screw feeder for the special case of operating with the device completely full of solid particles.

This work is divided into six chapters. In Chapter 1, a brief description of the screw feeder and an outline of study are presented. In Chapter 2, theoretical studies on the screw conveyor and feeder by previous workers are reviewed. In Chapter 3, the solid conveying mechanism is discussed and a new analytical treatment is presented. In Chapter 4, the experimental set up and the experimental procedure are described. Chapter 5 presents the computational procedure and discusses the treatment of data. Chapter 6 presents the results of the experiments and comparisons with theory along with the results of numerical parametric studies. Conclusions and suggestions for future work are presented in Chapter 7.

CHAPTER 2

LITERATURE REVIEW

Zimmer (1905, 1932) records that the Archimedan screw is undoubtedly the oldest type of screw conveyor. It was invented by Archimedes (287-212 BD) for pumping water and was probably used in the earliest flour mills. Morin (1956) reports that the first formula for determining the volumetric output (Q) of a screw was proposed by Prof. A. M. Samus in the late 19th century. The formula is given below;

$$Q = \eta \frac{\pi}{4} (D_b^2 - D_s^2) pN \qquad (2\text{-}1)$$

in which

D_b = outside screw diameter

D_s = screw root diameter

p = screw pitch

N = screw rpm

η = coefficient of loading

Q = volumetric output or delivery rate

This formula is simply a factor η times the sweep volume of the screw.

After the mechanization of farming methods, the enclosed screw conveyor (which is an important part of the combine harvester and the main device for bulk handling on farms and grain terminals) became the subject of increased study by agricultural engineers. The enclosed screw conveyor, which is similar to a screw feeder when it is operating under full capacity, has been tested experimentally by many workers (Wright, 1926a; Wright, 1926b; Konig et al., 1960; Millier, 1958; O'Callaghan, 1961; Fegan, 1959; Peart, 1958; Rehdugler, 1959a and 1959b; Stevens, 1962; Roberts and Willis, 1962.) Results of their experiments and observations indicate that:

(1) At low speeds of revolution (usually up to 200 rpm), the output per revolution is independent of rpm (i.e. the delivery is linearly proportional to rpm). (2) At higher rpms, the ouput volume per revolution declines with rpm and delivery will reach a maximum then decline. (3) The delivery of a screw at high rpm can be improved by elongating the intake part of the screw or force feeding (this indicates that under such condition the screw is running partial full and that the decline of output per revolution is caused by insufficient supply at the intake). (4) The delivery at a fixed rpm decreases with an increase in the angle of inclination of the screw to the horizontal. (5) Particles in a screw conveyor follow a helical path. The larger the helix angle formed, the better the volumetric efficiency (defined as the ratio of the volumetric feed rate to the sweep volume of the screw). (6) The helix angle formed by the movement of a particle in a vertical screw conveyor increases as the rpm increases. (7) The volumetric delivery rate of a screw varies with the type of material being transported. It also depends on other material characteristics such as moisture content that effect the coefficient of friction with the construction material of the feeder.

Some initial attempts have been made to theoretically analyze the screw conveyor by agricultural engineers. Anakin (1953) used Eqn. (2-1), and tried to find a general form for the coefficient of loading (η) from his experimental data. Without investigating the mechanism of conveying, the correlation he obtained is only limited to the conditions of his experiments. Morin (1956) developed a formula for a horizontal screw conveyor by a force analysis of a single particle in contact with the screw wing tip. The direction of movement of the particle was found from a force balance.

The relation between the direction of particle movement and velocity was also analyzed. From this information, and the assumption that all particles move at the same speed in the axial direction, an equation for the delivery rate was obtained. Though he didn't include the forces acting on the particle by the barrel surface and other particles, his analysis has led to the correct conclusion that the frictional coefficient of the particles on the screw affects the output.

Later works on the screw conveyor have employed similar approaches. Zaika (1958) worked on the combine harvester auger. Gutyar (1956), Thusing (1958), and Baks and Schmid (1960) developed equations for the output of vertical screw conveyors by including the weight of the particles in the analysis. These investigators also considered the frictional force arising from the centrifugal force of the particle on the barrel in their analyses. Vierling and Sinha (1960) also worked on a verticle screw conveyor and derived an equation for the critical speed (minimum speed to have particles moving upward).

Ross (1960) analyzed the force from particle stacks and derived equations for the inclined screw conveyor. His approach has a disadvantage in that it is very difficult to estimate the magnitude and direction of the forces on the particle of interest by adjacent particles. Without this information, the force balance is incomplete.

Concurrent with the efforts of the agricultural engineers, plasticating engineers were working on the theory of solid conveying in an extruder. Decker (1941) discussed the variables which control the solid delivery rate: the dimensions of the screw, the back pressure, and the coefficient of friction. He derived equations which can only be correlated qualitatively to experiments. He reached the conclusions that at a constant rpm the smaller

the friction between the plastic and the screw surface, the larger the friction between the plastic and the barrel surface, the larger the output rate. Weber (1947) treated the plastic in an extruder as a solid nut, but neglected the forces acting between the barrel and the material.

A much more realistic approach to the problem of solid conveying in a screw feeder is that given by Pawlowski (1949). He assumed that there is no internal shear in the solid and considered a balance of forces on the screw contents and the rotational movement caused by the torque. Maillefer (1952) derived an equation for the conveying rate in terms of the solid movement angle, but he neglected the channel curvature and didn't include all of the forces acting on the solid plug. Simonds (1952) introduced the concept of a balance of torques. His simplified treatment gives a result that the solid plug either turns with the screw or does not turn. This is far from the actual helical movement of the plug. Jackson et al. (1958) performed a similar analysis to that of Maillefer but included the normal force that the pushing flight exerts on the solid plug. However, they did not consider the forces exerted by the leading flight, and consequently their equations are not of much value.

The most thorough analysis was performed by Darnell and Mol (1956). They treated the particles as a solid plug and assumed that an isotropic pressure existed within the solid. They made a force balance in the axial direction and a torque balance about the screw axis to obtain an expression from which the solid movement angle at the barrel surface, and the conveying rate can be found. They also took into account the effect of back pressure. To simplify the treatment, an arithmetic average of the helix angle over the channel depth was used. This limited their analysis to a shallow channel screw. They also compared their theoretical

results with the experiment, but only by neglecting the friction forces caused by the solid pressure on both wings can the results give any reasonable agreement with the experiment. Tadmor and Klein (1970) modified this theory to include the case where the screw and barrel are made of different materials (i.e., have different coefficients of friction). They also illustrated the difficulty in obtaining an accurate result by Darnell and Mol's theory.

Metcalf (1965) developed an analysis by neglecting the back pressure, but considering the work needed to push the solid plug forward and to rotate the plug. He was able to derive an expression for the solid movement angle, but since he did not consider the work needed to conquer the frictional forces on the flights, the analysis is not satisfactory. Later workers on the solid conveying mechanism in a screw mainly followed the analysis of Darnell and Mol. Schneider (1969) changed the isotropic pressure assumption. The mean pressure (P) was taken as reference and the pressure at other surfaces were assumed proportional to this pressure. Broyer and Tadmor (1972) derived equations allowing for a variable channel depth and allowing for a pressure dependent density. Lovegrove (1973) reported his observation that for the most part in an extruder, shearing within the loose polymer powder may be neglected and that the loose solids move like a solid plug. Lovegrove and Williams (1972) (1973) (1974) added the effect of gravity forces to the Schneider's modified equations.

Recent developments in coal gasification demand a high pressure feeding device. The screw feeder is one of the considerations. In technical progress reports of ERDA, Mistry (1976, 1977) stated that the screw feeder was capable of operating under a back pressure of 1000 psi. A decline of the feed rate with the back pressure was observed. The declination varied

with types of coal used. A computer simulation based upon Darnell and Mol's theory of the feed rate and power needed for different operation condition had been studied. No comparison of experimental data and the simulation was made.

Darnell and Mol's analysis gives a reasonable explanation of the solid conveying mechanisms, but the analysis only applies to a shallow channel screws. Unfortunately the predictions usually do not agree very well with experiments. In this study, a model which considers a more general case and can be applied a channel of an arbitrary depth has been developed. In addition, the major assumption in Darnell and Mol's treatment, that the pressure is uniform across the channel for a small solid plug, has been reconsidered.

CHAPTER 3

ANALYSIS OF SOLID CONVEYING MECHANISM

3.1 THE GEOMETRY OF THE SCREW-FEEDER

A screw feeder or extruder often has a single screw carrying one or two wings, rotating in a tightly fitted barrel. Typically, the device is horizontal or slightly inclined. Material is fed without restriction to one end of the screw from a hopper and delivered at the other end.

Figure 3.1 illustrates the geometric features of a single wing screw. A single wing screw has been chosen for the purpose of simplicity. The inner diameter of the barrel is D_b, and the diameter of the screw root is D_s. The radial clearance between the crest of the screw wing and the inner barrel surface is δ_c. The axial distance of one full turn of the screw is termed the pitch, p, and the axial direction between wings is the channel width, H. The thickness of the screw wing in the axial direction is E. The angle formed between a plane parallel to the wing surface at any point and a plane normal to the screw axis (or the plane of motion) is called the helix angle $\alpha(r)$. At the wing tip the helix angle is α_b and at the wing root the helix angle is α_s.

To simplify the treatment, the screw considered in the analysis is assumed to have constant pitch, wing thickness, channel width, barrel diameter and screw root diameter. The clearance δ_c is assumed negligible. Consequently, the diameter of the screw wing is identical to D_s.

The helix angle will vary with radial position from the screw axis as illustrated in Fig. 3.1. Mathematically the helix angle can be related to the pitch and radius. This relation has been given by Tadmor & Klein (1970) and will be reviewed here. Assume that the wing tip of

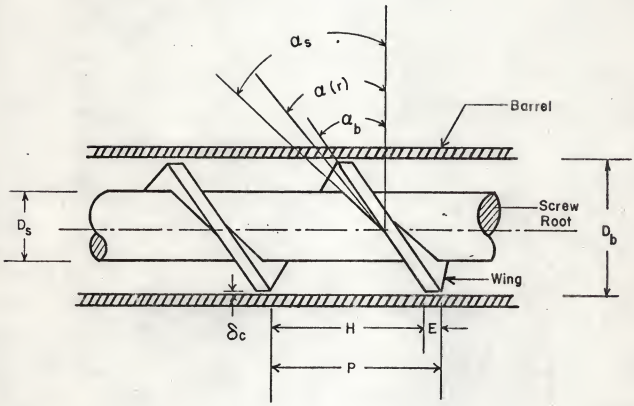

Figure 3.1. Geometry of screw.

a screw is painted with ink and the screw is placed on a piece of paper and rotated one full turn. The paths traced on the paper are shown in Fig. 3.2.

It can be seen that the helix angle at the wing tip, α_b, can be expressed as

$$\tan \alpha_b = \frac{p}{\pi D_b} \tag{3.1}$$

Now if the radius of the wing is reduced to r, then the trace of one full turn in the axial direction will still be p, but that, in the tangential direction will be $2\pi r$. Therefore, the helix angle α will be

$$\tan \alpha = \frac{p}{2\pi r} \tag{3.2}$$

This is the general expression for the helix angle. Similarly, the angle at the screw root is:

$$\tan \alpha_s = \frac{p}{\pi D_s} \tag{3.3}$$

3.2 CONVEYING MECHANISM

To understand the solid conveying mechanism in a screw feeder, it is easiest to begin with a simple model. Consider a rigid solid element confined between two infinite parallel plates. The lower plate is stationary, and the upper one moves at a constant velocity V as shown in Fig. 3.3. The coefficient of friction and the contact area between the element and the moving upper plate are, respectively, f_b and A_b, while those between the plug and lower plate are f_s and A_s. If the pressure exerted by the solid element on the plates is equal, then the friction force that the upper plate exerts on the plug in the direction of movement is given by $F_b = PA_b fb$. The force that the upper plate exerts on the plug in the direction of movment is given by $F_b = PA_b fb$. The force that the lower plate exerts on the plug in the opposite direction is $F_s = PA_s f_s$. There

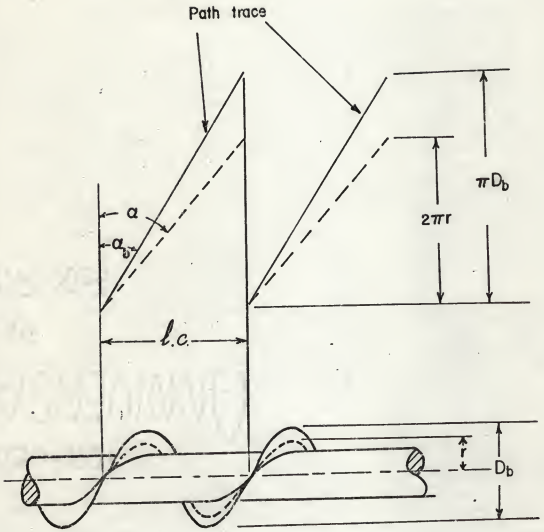

Figure 3.2. Trace of the screw wing tips rotated on a flat plane.

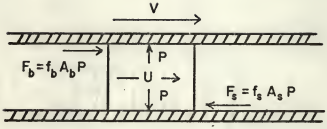

Figure 3.3. Motion of a solid plug confined between two flat planes.

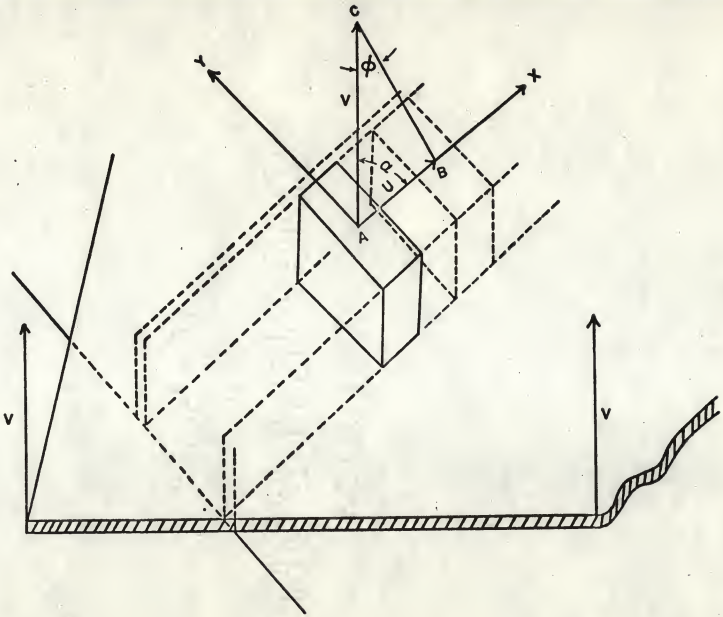

Figure 3.4. Motion of a solid plug confined between a rectangular channel and a flat plane.

are three possible results: 1) If $F_s < F_b$, the plug will accelerate until it reaches the velocity of upper plate, 2) If $F_s > F_b$, the plug will stop after some time, 3) If $F_s = F_b$, the plug will move with a constant velocity u such that $1 \leq u \leq V$.

Now consider the constraint of the screw wing to the solid plug movement. To approximate this case, consider the solid plug to be confined in a rectangular channel fixed to the lower plate. Again the upper plate moves at a constant velocity of V and at an angle α to the down channel direction as shown in Fig. 3.4. The magnitude of the force exerted by the upper moving plate on the solid plug is still $A_b f_b P$. The solid plug tends to move in the direction of the motion of the plate, but as a consequence of the presence of the channel, it can only slide in the down channel direction at a certain velocity, u.

For the system described above, a solid plug is confined in a channel and is moving at velocity u because of the sliding upper plate. At some time t, the center of the solid plug is at position A. At another time $t = \Delta t$ this point moves to a new position B in the down channel direction. The point on the upper plate contact with point A at time t is at another position C at time $t + \Delta t$ as shown in Fig. 3.4. The magnitudes of V and u can be expressed by the length of the lines, AC and AB, respectively. The relative motion of the solid plug with respect to the plate can be expressed by the line, CB. The angle between the lines AC and CB is defined as the solid movement angle relative to the plate(ϕ). This angle is an important quantity for the evaluation of the feed rate of a screw. From Fig. 3.4 it can be seen that for a constant upper plate velocity of V, the faster the solid plug moves in the down channel direction the larger the angle ϕ.

How fast the solid plug moves is determined by the forces acting on it. The force against the movement will come from the friction force on the channel. The force to push it forward in this case comes from the friction force of the upper plate.

The actual conveying mechanism of a screw feeder is more complicated than the simple model presented above because of its curvature. But, in principle, the mechanism is quite similar to the simple model. The solid material is assumed to fill all the available space between the screw and barrel wall. Rotation of the screw tends to rotate the ribbon of solid in the radial direction. Friction on the barrel wall opposes this motion. The ribbon can avoid rotation by moving axially, though this is also opposed by the friction on the barrel wall and on the screw. The ribbon, therefore, moves both in rotation and axially so that effort against the friction is a minimum.

It should, therefore, be possible to quantitatively predict the performance of a screw feeder from a knowledge of its dimensions and the coefficients of friction involved with the aid of the concepts and assumptions discussed in the first two sections of this chapter.

3.3 DELIVERY RATE

The relation between the delivery rate and the angle of solid movement ϕ has been discussed by Darnell and Mol. (1956) and other workers. Here the same expression for the delivery rate in terms of solid movement angle will be outlined.

Consider a solid element in the screw as shown in Fig. 3.5. It has an unknown velocity in the axial direction, V_{pa}. This velocity is independent of channel depth and axial position because the element is assumed to be rigid and does not undergo deformation. The volumetric delivery

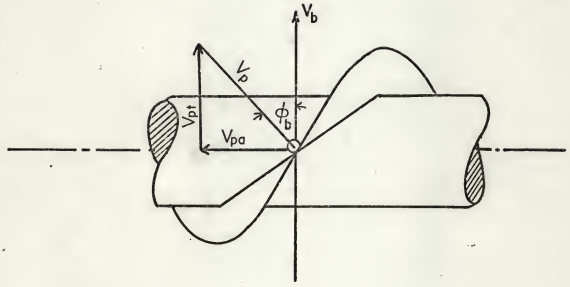

Figure 3.5. Velocity of a solid element in the screw channel.

rate of the screw is obtained by multiplying this velocity by the cross sectional area of the plug:

$$Q = V_{pa}\,\pi(R_b^2 - R_s^2)\,(p - E)/p \qquad (3\text{-}4)$$

where R_b and R_s are the radius at the inner barrel surface and that at the screw root respectively, p is the pitch of the screw, and E is the wing thickness. The last term represents the fraction of the cross sectional area occupied by the wing.

Consider a point of a solid plug in contact with the wing, as shown in Fig. 3.6. When the screw wing tip moves a small distance from A to A', the element moves from A to B', still in contact with the wing tip. The angle of this movement with respect to the plane normal to the screw axis is the solid movement angle at barrel surface, ϕ_b. The lengths of lines AA', AB', AC, and B'C represent the magnitudes of V_b, V_p, V_{pt} and V_{pa}, respectively. The axial component of the velocity, v_{pa}, is AB' $\sin\phi_b$. From Fig. 3.6 it can be shown that the following relationship holds for the angle ϕ_b.

$$\tan\phi_b = \frac{B'C}{AA' - AB'\sin\phi_b/\tan\alpha_b} \qquad (3\text{-}5)$$

Rearrangement of Eqn. (3-5) gives

$$\frac{B'C}{AA'} = \frac{\tan\phi_b\,\tan\alpha_b}{\tan\phi_b + \tan\alpha_b} \qquad (3\text{-}6)$$

where B'C/AA' represents the ratio between the axial velocity of the element at the wing tip (V_{pa}) to the wing tip speed of revolution (V_b)

$$\frac{B'C}{AA'} = \frac{V_{pa}}{V_b} \qquad (3\text{-}7)$$

Then V_{pa} is obtained as

$$V_{pa} = V_b \frac{\tan \phi_b \tan \alpha_b}{\tan \phi_b + \tan \alpha_b} \tag{3-8}$$

Substituting the above equation into Eqn. (3.4) and equating V_b to the perimeter times speed of revolution ($V_b = \pi N D_b$) gives an expression for the volumetric delivery in terms of measurable quantities and the angle ϕ_b:

$$Q = \pi N D_b \frac{\tan \phi_b \tan \alpha_b}{\tan \phi_b + \tan \alpha_b} [\frac{\pi}{4} (D_d^2 - D_s^2) \frac{p-E}{p}] \tag{3-9}$$

If the frictional force between the solid element and the screw is so large that the particles in fact adhere to the screw, the plug will not move with respect to the screw, i.e., $\phi_b = 0$ and $V_{pa} = 0$, as well as $Q = 0$. If the frictional froce between the plug and screw is negligible, this results in the maximum delivery rate and the angle $\phi_b = 90 - \alpha_b$. In all real cases, the angle will be in range $0 < \phi_b < 90 - \alpha_b$. A higher delivery rate can be achieved if the friction coefficient between the barrel and solid plug is very large compared to that between the screw and solid plug. Theoretically, the upper limit of ϕ_b is 90°. In this case the volumetric feed rate equals the sweep volume of the screw. This would be the case when the plug moves like a nut held in a wrench.

3.4 ANALYSIS OF FORCE AND WORK

If the angle ϕ_b can be determined, then the delivery rate can be calculated from Eqn. (3-9). A force and torque balance is used to obtain an expression for the angle ϕ_b.

The basic assumptions that have been introduced in the derivation are:

(1) The solid particles in the channel behave as a rigid body.

(2) Solid particles fill up all of the available space in the channel.

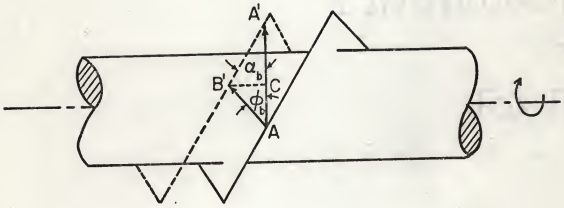

Figure 3.6. Motion of a particle in contact with the rotating screw wing tip.

(3) The geometry of the screw does not change with axial position.

(4) The clearance between the wing tip and the barrel is negligible.

(5) The coefficient of friction is constant for any surface but may be different for different surfaces in the device (i.e. barrel, wing, root).

(6) Gravitational forces and centrifugal forces are negligible.

(7) The bulk density of particles in the channel is constant. This is implied by previous assumptions.

(8) There is no pressure difference between the inlet and outlet of the screw; in other words, there is no back pressure. At the end of this chapter, an expression to consider the case of back pressure is also derived.

Consider a wedge-shaped element (strictly speaking this is not wedge shape as a result of the variation of α with radial position) that extends from the screw root to the barrel surface, as shown in Fig. 3.7 a and b. Under steady operation this element will move at a constant speed in a helical path toward the exit of the screw and form an angle ϕ_b between the direction of movement at the surface in contact with the barrel and the surface perpendicular to the screw axis, as shown in Fig. 3.8.

Since the element is traveling under constant speed without changing its kinetic energy and potential energy the toatl work done by all forces acting on the elementwhen it travels from one position to another position must be zero:

$$\sum_{i=1}^{n} W_i = 0 \tag{3-10}$$

Each force can be divided into the axial and tangential components. F_{ia} and F_{iT}, respectively, similarly, the corresponding displacement can be divided into the axial and tangential components, ℓ_{ia} and ℓ_{iT}, respectively. The work W_i done by the force F_i when the element travels a distance ℓ_i can be expressed as:

$$W_i = F_{ia}\ell_{ia} + F_{iT}\ell_{iT} \tag{3-11}$$

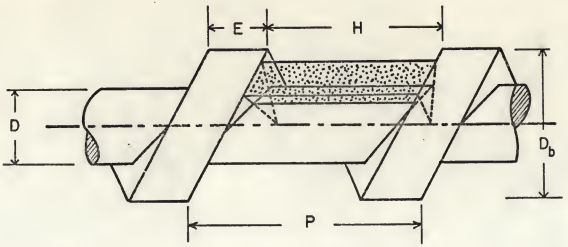

Figure 3.7. (a) Geometry of the 'wedge' shape element.

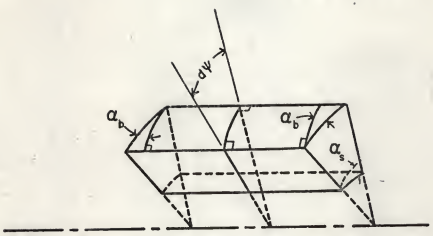

Figure 3.7. (b) Enlarged view of a 'wedge' shape element.

Defining

$$W_{ia} = F_{ia} \ell_{ia} \tag{3-12}$$

$$W_{iT} = F_{iT} \ell_{iT} \tag{3-13}$$

and summing over all contributions gives

$$\sum_{i=1}^{n} W_i = \sum_{i=1}^{n} F_{ia} \ell_{ia} + \sum_{i=1}^{n} F_{iT} \ell_{iT}$$

$$= \sum_{i=1}^{n} W_{ia} + \sum_{i=1}^{n} W_{iT} \tag{3-14}$$

For the element to travel a unit length at the barrel surface, in the direction of ϕ_b, any point in the element will travel axially a distance $\ell_a = \sin \phi_b$, but the tangential movement of each point will be a function of radius $\ell_T = r/R_b \cos \phi_b$ as shown in Fig. 3-9. Consequently Eqn. (3-14) can be expressed as

$$\sum_{i=1}^{n} W_i = \ell_a \sum_{i=1}^{n} F_{ia} + \sum_{i=1}^{n} F_{iT} \ell_{iT} \tag{3-15}$$

Since there is no acceleration in the axial direction, the sum of all the forces in the axial direction should be zero:

$$\sum_{i=1}^{n} F_{ia} = 0 \tag{3-16}$$

This relation implies that

$$\sum_{i=1}^{n} W_{ia} = \ell_a \sum_{i=1}^{n} F_{ia} = 0 \tag{3-17}$$

consequently

$$\sum_{i=1}^{n} W_{ir} = \sum_{i=1}^{n} W_i - \sum_{i=1}^{n} W_{ia} = 0 \tag{3-18}$$

Figure 3-8 shows the forces acting on the wedge element, F_1 is the friction force between the barrel surface and the elment, and it forms an angle ϕ_b with a plane normal to the axis of the screw. The force F_1 can be

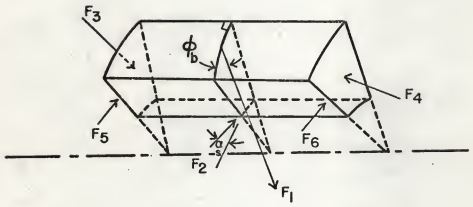

Figure 3.8. Forces acting on a solid element.

expressed in terms of the average pressure $\bar{P}_b$, the coefficient of friction f_b and the area over which it acts:

$$F_1 = \bar{P}_b H R_b d\psi f_b \tag{3-19}$$

where $H = p - E$ is the channel width of the screw and ψ is the angular coordinate.

F_1 may be expressed in terms of its components: The component acting in the axial direction is,

$$F_{1a} = F_1 \sin \phi_b \tag{3-20}$$

and the component acting in the tangential direction is,

$$F_{1T} = F_1 \cos \phi_b$$

The work done by this force is equal to the force times distance it travels for a unit displacement at the barrel surface

$$W_{1a} = -F_1 \sin^2 \phi_b \tag{3-22}$$

and

$$W_{1T} = -F_1 \cos^2 \phi_b \tag{3-23}$$

here the minus sign appears as the result of the opposite direction of force and movement.

F_2 is the friction force on the screw root:

$$F_2 = \bar{P}_s CHR_s d\psi f_s \tag{3-24}$$

where $\bar{P}_s$ is the average pressure exerted by the element on the screw root. Here C is the ratio of R_s to R_b, and f_s is the coefficient of friction of the element on the screw root.

The direction of the friction force is opposite to the relative movement of the contact surface. Since the solid element can only move in the direction of the channel relative to the screw. The force acting

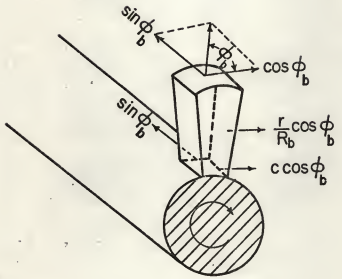

Figure 3.9. Displacement in a solid element for a unit displacement at the barrel surface.

on the solid element by the screw root is in the direction of the channel at the screw root, whcih has an angle, α_s, with the plane normal to the screw axis.

F_2 can be broken into the axial and tangential components:

$$F_{2a} = F_2 \sin \alpha_s \tag{3-25}$$

$$F_{2T} = F_2 \cos \alpha_s \tag{3-26}$$

where α_s is the wing angle to the direction normal to the axis of screw at the screw root. The movement of this surface axially is sin ϕ_b, and tangentially is C cos ϕ_b as shown in Fig. 3-9. Consequently, the work will be:

$$W_{2a} = -F_{2a} \sin \phi_b \tag{3-27}$$

and

$$W_{2T} = F_{2T} \cos \phi_b \tag{3-28}$$

At the pushing wing and the leading wing, there are pressures, P* and P_w respectively, exerted by the wings normal to the element. It is assumed that P* and P_w are uniformly distributed on the wing surface and independent of radius (direction of the normal changes over the surface).

Now consider the surface of the leading wing in contact with the wedge element, and a subelement of this surface of width dr at radius r (as shown in Fig. 3-10). The force acting on the subelement is:

$$dF_3 = P_w dA$$

The area of this strip dA is equal to length of the strip times dr. The length of the strip as shown in Fig. 3-9 is approximately r $d\psi/\cos \alpha$. The Eqn.(3-29) can be rewritten as:

$$dF_3 = P_w \frac{r d\psi}{\cos \alpha} dr \tag{3-30}$$

This force is normal to the wing surface, and it can be divided into the axial and tangential components:

$$dF_{3a} = -P_w \frac{r d\psi}{\cos \alpha} dr \cos \alpha \tag{3-31}$$

$$= -P_w R_b d\psi dr$$

$$dF_{3T} = -P_w \frac{r d\psi}{\cos \alpha} dr \sin \alpha \tag{3-32}$$

$$= -P_w R_b \, d\psi dr \tan \alpha$$

This small strip will move axially a distance $\sin \phi_b$ and tangentially $r/R_b \cos \phi_b$ when the solid element moves a unit distance at the barrel surface. The components of work associated with this movement are:

$$dW_{3a} = dF_3 \sin \phi_b \tag{3-33}$$

$$= -P_w r d\psi dr \sin \phi_b$$

$$dW_{3T} = dF_{3T} \sin \phi_b \frac{r}{R_b} \tag{3-34}$$

$$= -P_w \, r d\psi \tan \alpha \frac{r}{R_b} dr$$

Integration from $r = R_s$ to $r = R_b$ gives the work done by the normal force of the leading fright on the element

$$W_{3a} = \int_{R_s}^{R_b} dW_{3a} \tag{3-35}$$

$$= \frac{1}{2} P_w R_b^2 (1 - C^2) \, d\psi \sin \phi_b$$

$$W_{3T} = \int_{R_s}^{R_b} dW_{3T} \tag{3-36}$$

$$= \frac{1}{2} P_w R_b^2 (1 - C^2) \tan \alpha_b \, d\psi \cos \phi_b$$

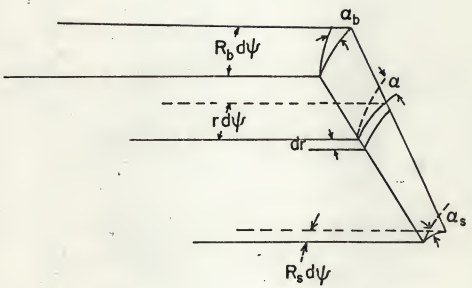

Figure 3.10. Side view of the solid element in contact with the screw wing.

Using a parallel treatment, one can obtain the work done by the normal force by the pushing wing on the element:

$$W_{4a} = \frac{1}{2} P^* R_b^2 (1 - C^2) \, d\psi \sin \phi_b \tag{3-37}$$

$$W_{4T} = \frac{1}{2} P^* R_b^2 (1 - C^2) \, d\psi \tan \alpha_b \cos \phi_b \tag{3-38}$$

where f_w is the coefficient of friction of the element on the wing. The friction force can be broken into axial and tangential components: There are also friction forces accompanying the normal forces. They have the direction parallel to wing and with magnitudes:

$$dF_5 = f_w dF_3 \tag{3-39}$$

$$dF_6 = f_w dF_4 \tag{3-40}$$

These forces have axial and tangential component given:

$$dF_{5a} = -dF_5 \sin \alpha = -f_w dF_3 \sin \alpha \tag{3-41}$$

$$dF_{6a} = -f_w dF_4 \sin \alpha \tag{3-42}$$

$$dF_{5T} = f_w dF_3 \cos \alpha \tag{3-43}$$

$$dF_{6T} = f_w dF_4 \cos \alpha \tag{3-44}$$

Multiplying the above forces by distances they travel followed by integration from $r = R_s$ to $r = R_b$ gives:

$$W_{5a} = -P_w R_b^2 (1 - C) \tan \alpha_b \, d\psi f_w \sin \phi_b \tag{3-45}$$

$$W_{6a} = -P^* R_b (1 - C) \tan \alpha_b \, d\psi f_w \sin \phi_b \tag{3-46}$$

$$W_{5T} = \frac{1}{3} P_w R_b^2 (1 - C^2) \, d\psi f_w \cos \phi_b \tag{3-47}$$

$$W_{6T} = \frac{1}{3} P^* R_b (1 - C^3) \, d\psi f_b \cos \phi_b \tag{3-48}$$

Equations (3-23), (3-28), (3-36), (3-38), (3-47), and (3-48) can be substituted into the axial work balance, Eqn. (3-17), to obtain

$$\overline{P_b}\, H\, R_b\, d\psi\, f_b \sin^2 \phi_b + \overline{P_s}\, C H R_b\, d\psi\, f_s \sin \alpha_s \sin \phi_b$$

$$+ \frac{1}{2} P_w R_b^2 (1 - C^2)\, d\psi \sin \phi_b + (P_w + P^*) R_b^2 (1 - C) \tan \alpha_b\, d\psi\, f_w$$

$$= \frac{1}{2} P^* R_b^2 (1 - C^2)\, d\psi \sin \phi_b \qquad (3\text{-}49)$$

Rearrangement of Eqn. (3-49) results in

$$\overline{P_b}\, H f_b \sin \phi_b + \overline{P_s}\, C H f_s \sin \alpha_s + \frac{1}{2} P_w R_b^2 (1 - C^2)$$

$$+ (P^* + P_w) R_b (1 - C) f_w \tan \alpha_b = \frac{1}{2} P^* R_b (1 - C^2) \qquad (3\text{-}50)$$

Defining:

$$A_1' = H f_b \qquad (3\text{-}51)$$

$$A_1 = \overline{P_b} A_1' \qquad (3\text{-}51')$$

$$A_2' = C H f_s \sin \alpha_s \qquad (3\text{-}52)$$

$$A_2'' = \frac{1}{2} R_b (1 - C^2) \qquad (3\text{-}53)$$

$$A_2''' = R_b (1 - C) \tan \alpha_b f_w \qquad (3\text{-}54)$$

$$A_2 = \overline{P_b} A_2' + P_w (A_2'' + A_2''') \qquad (3\text{-}55)$$

$$A_3' = \frac{1}{2} R_b (1 - C^2) - A_2''' \qquad (3\text{-}56)$$

Introducing Eqns. (3-51, 55, 56) into Eqn. (3-49) and rearranging gives

$$P^* = \frac{(A_1 \sin \phi_b + A_2)}{A_3'} \qquad (3\text{-}57)$$

Substituting Eqns. (3-23), (3-28), (3-36), (3-38), (3-47), (3-48) into Eqn. (3-18), one obtains:

$$\overline{P_b}\, H R_b\, d\psi\, f_b \cos^2\phi_b - \overline{P_s}\, C^2\, H R_b\, d\psi\, f_s \cos\alpha_s \cos\phi_b$$

$$+ \frac{1}{2} P_w (1 - C^2) R_b^2 \tan\alpha_b\, d\, \cos\phi_b - \frac{1}{3}(P^* + P_w) \qquad (3\text{-}58)$$

$$R_b^2 (1 - C^3)\, d\psi\, f_w \cos\phi_b - \frac{1}{2} P^* (1 - C^2) R_b^2 \tan\alpha_b\, d\psi \cos\phi_b = 0$$

Rearrangement of the above equation gives:

$$\overline{P_b}\, H f_b \cos\alpha_b - \overline{P_s}\, H C^2 f_s \cos\alpha_s + \frac{1}{2} P_w R_b (1 - C^2) \tan\alpha_b$$

$$- \frac{1}{3}(P_w + P^*) R_b (1 - C^3) f_w = \frac{1}{2} P^* R_b (1 - C^2) \tan\alpha_b \qquad (3\text{-}59)$$

Defining:

$$B_1' = f_s C^2 H \cos\alpha_s \qquad (3\text{-}60)$$

$$B_1 = \overline{P_s} B_1' \qquad (3\text{-}61)$$

$$B_2' = \frac{1}{2}(1 - C^2) \tan\alpha_b R_b \qquad (3\text{-}62)$$

$$B_2 = P_w B_2' \qquad (3\text{-}63)$$

$$B_3' = \frac{1}{3} R_b (1 + C^3) f_w \qquad (3\text{-}64)$$

$$B_3 = P_w B_3' \qquad (3\text{-}65)$$

$$B_4'' = \frac{1}{2} R_b (1 - C^2) \tan\alpha_b \qquad (3\text{-}66)$$

$$B_4' = B_3' + B_4'' \qquad (3\text{-}67)$$

Substituting Eqns. (3-60) through (3-67) into Eqn. (3-59) and rearranging gives:

$$P^* = (A_1 \cos\phi_b - B_1 + B_2 - B_3) / B_4' \qquad (3\text{-}68)$$

Equating Eqn. (3-50) and Eqn. (3-68) to eliminate P* gives

$$(A_1 \cos\phi_b - B_1 + B_2 - B_3) / B_4' = (A_1 \sin\phi_b + A_2) / A_3' \qquad (3\text{-}69)$$

Now define

$$K = \frac{B_4'}{B_3'} \qquad (3\text{-}70)$$

Rearrangement of Eqn. (3-69) followed by substitution of Eqn. (3-70) gives an expression for the angle of solid movement

$$\cos \phi_b = K \sin \phi_b + [KA_2 + B_1 - B_2 + B_3] / A_1 \qquad (3\text{-}71)$$

Substituting Eqns. (3-51) through (3-56) and (3-61) through (3-67) into Eqn. (3-71) yields an expression for the angle ϕ_b in terms of screw geometry, coefficients of friction, and the pressure on each surface

$$\cos \phi_b = K \sin \phi_b + K\{\frac{f_s}{f_b}\frac{\bar{P}_s}{\bar{P}_b} C \sin \alpha_s + \frac{R_b}{H}\frac{P_w}{P_b}[\frac{1}{2} \cdot \frac{1}{f_b}(1 - C^2)$$

$$+ \frac{f_w}{f_b} \tan \alpha_b \, (1 - C)]\} + \frac{f_s}{f_b}\frac{\bar{P}_s}{\bar{P}_b} C^2 \sin \alpha_s + \frac{1}{3}\frac{f_w}{f_b}\frac{P_w}{\bar{P}_b}\frac{R_b}{H}(1 - C^3)$$

$$- \frac{1}{2}\frac{R_b}{H}\frac{P_w}{\bar{P}_b} \tan \alpha_b \, (1 - C^2) \qquad (3\text{-}72)$$

From Eqn. (3-71) the angle ϕ_b can be calculated if the ratios of P_w to $\bar{P}_b$ and $\bar{P}_s$ to $\bar{P}_b$ are known. An analysis of the pressure gradient in the solid element will provide this information.

3.5 PRESSURE DISTRIBUTION IN A SOLID ELEMENT

The actual solid pressure distribution in the cross channel direction in the screw channel is difficult to analyze. Here a simplified model which neglects the variation of α over the wing is used to estimate the pressure distribution.

Consider a screw channel which the variation of α has been neglected, it has an angle $\bar{\alpha}$ to the plane normal to screw axis. Here the angle $\bar{\alpha}$ is the weight average of the helix angle. Consider a solid element which is confined between two wings and is perpendicular to the channel as shown in Fig. 3-11. (Note: the orientation of this element is different from the element in the previous treatment.) The width of this element is dZ_b at the barrel surface, and shrinks to dZ_s at the screw root. The relation between dZ_b and dZ_s is:

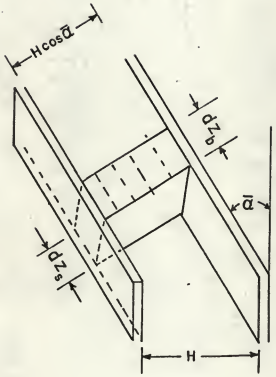

Figure 3.11. Geometry of the solid element for pressure distribution in analysis.

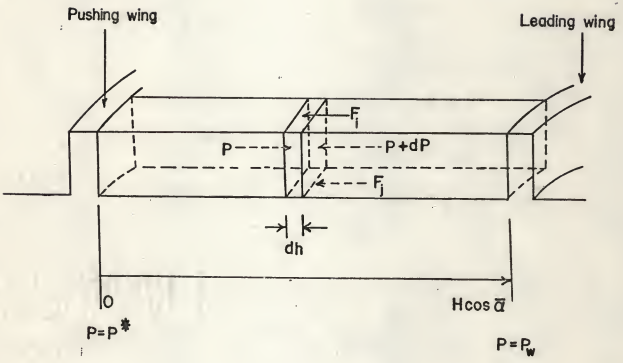

Figure 3.12. Forces and pressures acting on a small section of the solid element.

$$dZ_s = CdZ_b \tag{3-73}$$

It is assumed that the pressure in the solid element can only vary over the length of the element and is independent of the radial position. The dotted lines in Fig. 3-11 show the equal pressure lines. For a subelement as shown in Fig. 3-12 at position h with length dh, the pressure acting at each face is P and P + dP respectively. There are also friction forces acting on it at the surfaces in contact with barrel and the screw root. The magnitude of the components acting perpendicular to the channel are dF_i and dF_j respectively. A force balance gives

$$PdA = dF_i + dF_j + (P + dP)dA \tag{3-74}$$

where dA is the trapezoidal cross sectional area of the solid element, and can be expressed as:

$$\begin{aligned} dA &= \frac{1}{2}(R_b - R_s)(dZ_b + dZ_s) \\ &= \frac{1}{2}(1 - C^2) R_b{}^2 dZ_b \end{aligned} \tag{3-75}$$

Now dF_i and dF_j can be expressed in terms of the local pressure acting on the barrel surface as;

$$F_i = P_b f_b \sin(\phi_b + \bar{\alpha})\, dZ_b dh \tag{3-76}$$

and

$$dF_j = P_s f_s \sin(\alpha_s - \bar{\alpha})\, dZ_s dh \tag{3-77}$$

substituting Eqns. (3-75), (3-76) and (3-77) into Eqn. (3-74) gives;

$$\begin{aligned} dp[\tfrac{1}{2}(1 - C^2)R_b] = &- (P_b f_b \sin(\phi_b + \bar{\alpha}) \\ &+ P_s(f_s \sin(\alpha_s - \bar{\alpha})dh) \end{aligned} \tag{3-78}$$

Previously it was assumed that $P_b = P_s$. In addition if we assume a linear relationship between P and P_b, P_s; then

$$P_b = P_s = k_p P \tag{3-79}$$

By introducing Eqn. (3-79) into Eqn. (3-78), one obtains:

$$\frac{1}{2}\frac{dP}{P}(1 - C^2)\, R_b = k_p\,(f_b \sin(\phi_b + \bar{\alpha}) + Cf_s \sin(\alpha_s - \bar{\alpha})\,dh) \tag{3-80}$$

Integration of Eqn. (3-80) and using the boundary condition at h = 0, i.e., P = P*, one obtains:

$$P = P^* \exp\,[-k_p h \cos\bar{\alpha}\,(f_b \sin(\phi_b + \bar{\alpha}) + Cf_s \sin(\alpha_s - \bar{\alpha})]/[\tfrac{1}{2}(1 - C^2)\, R_b] \tag{3-81}$$

Since P_w is the pressure at h = H cos $\bar{\alpha}$, one has

$$P_w = P^* \exp\,[-k_p H \cos\bar{\alpha}\,(f_b \sin(\phi_b + \bar{\alpha}) + Cf_s \sin(\alpha_s - \bar{\alpha})]/[\tfrac{1}{2}(1 - C^2)\, R_b] \tag{3-82}$$

P_b or P_s can be calculated by average over the length of the element:

$$\bar{P}_b = \bar{P}_s = \frac{\int_0^{H\cos\bar{\alpha}} P_b\, dh}{H \cos\bar{\alpha}} \tag{3-83}$$

After the integration the result is:

$$\overline{P_b} = \overline{P_s} = \frac{1}{H\cos\alpha}\,\frac{2(1 - C^2)R_b\,(P^* - P_w)}{f_b \sin(\phi_b + \bar{\alpha}) + Cf_s \sin(\alpha_s - \bar{\alpha})} \tag{3-84}$$

Eqns. (3-82) and (3-83) supply the information to calculate $\bar{P}_b$, $\bar{P}_s$ and P_w. The ratio of P_w to $\bar{P}_b$ can be obtained by dividing Eqn. (3-82) by Eqn. (3-84), and the P* term will cancel out. This ratio can be used to solve for ϕ_b from Eqn. (3-72).

3.6 EFFECT OF BACK PRESSURE

If a pressure difference exists over the length of the barrel, then there will be one more force that needs to be considered in the analysis. Consider

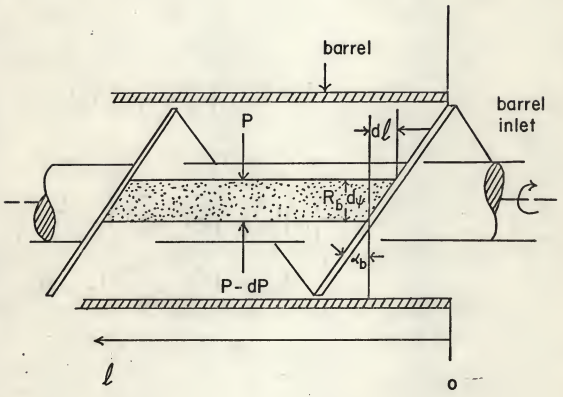

Figure 3.13. The solid element with a pressure difference acting on it and geometric relation between dψ and dℓ.

again the solid element used in section 3.4 (see Fig. 3.13). With reference to Fig. 3-13, let the mean pressure difference in the wedge shape solid element be $d\bar{P}$, since pressure is normal to the surface, the force it forms acting tangent to the axial direction on a small strip on the side wall of the solid element at a radius r will be

$$dF_{7T} = d\bar{P}\ H\ rdr \tag{3-85}$$

The movement of this strip will be $r/R_b \cos \phi_b$ tangentially when the surface contact will barrel moves a unit distance. Then the work done by this force will be:

$$dW_{7T} = dF_7 \frac{r}{R_b} \cos \phi_b$$

$$- d\bar{p}H \frac{r^2}{R_b} \cos \phi_b\ dr \tag{3-86}$$

Integration from $r = R_s$ to $r = R_b$ gives:

$$W_{7T} = \int_{R_s}^{R_b} d\bar{p}\, H \frac{r^2}{R_b} \cos \phi_b\ dr$$

$$= \frac{1}{2} d\bar{p}\ H\ R_b\ (1 - C^2) \cos \phi_b \tag{3-87}$$

Addition of this term to the RHS of Eqn. (3-18), followed by the rearrangement and combination with Eqn. (3-57) gives a modified expression for the angle of solid movement

$$\cos \phi_b = K \sin \phi_b + [KA_2 + B_1 - B_2 + B_3 + B_5]/A_1 \tag{3-88}$$

where

$$B_5 = \frac{1}{2} H\ (1 - C^2) \frac{d\bar{P}}{d\psi} \tag{3-89}$$

represents the contribution of a pressure difference on the delivery rate.

It is inconvenient to use angle ψ in the delivery rate expression and it is easier to express ψ in terms of distance from the barrel inlet (ℓ).

From Fig. 3-13 it can be seen that the relationship between ψ and ℓ is

$$\tan \alpha_b \, R_b \, d\psi = d\ell \tag{3-90}$$

or

$$d\psi = \frac{d\ell}{\tan \alpha_b \, R_b} \tag{3-91}$$

Then B_5 can be expressed in terms of $d\ell$ as:

$$B_5 = \frac{1}{2} H (1 - C^2) \tan \alpha_b \, R_b \frac{d\bar{P}}{d\ell} \tag{3-92}$$

Making use of Eqns. (3-51) through (3-56) and (3-60) through (3-67) permits the expression for $\cos \phi_b$ to be written as:

$$\cos \phi_b = K \sin \phi_b + \{K[A_2 \frac{\overline{P_S}}{P_b} + (A_2'' + A_2''') \frac{P_w}{P_b}]$$

$$+ B_1' \frac{\bar{P}_S}{P_b} - B_2' \frac{P_w}{P_b} + B_3' \frac{P_w}{P_b}\} / A_1 + \frac{B_5'}{A_1} \frac{d\bar{P}}{d\ell P_b} \tag{3-93}$$

where

$$B_5' = \frac{1}{2} H (1 - C^2) \tan \alpha_b \, R_b \tag{3-94}$$

With the assumption that $\bar{P} = P_b = \bar{P}_A$, Eqn. (3-94) becomes:

$$\cos \phi_b = K \sin \phi_b + \{K[A_2' + (A_2'' + A_3''') \frac{P_w}{P_b}] \quad .$$

$$+ B_1' + (B_3' - B_2') \frac{P_w}{P_b}\} / A_1' + \frac{B_5'}{A_1'} \frac{d \ln \bar{P}}{d\ell} \tag{3-95}$$

or

$$\frac{B_5'}{A_1'} \frac{d \ln \bar{P}}{d\ell} = \cos \phi_b - K \sin \phi_b - M \tag{3-96}$$

where

$$M = \{K[A_2' + (A_2'' + A_3''') \frac{P_w}{P_b}]$$

$$+ B_1' + (-B_2' + B_3') \frac{P_w}{P_b}\} / A_1' \tag{3-97}$$

Integration of Eqn. (3-96) gives:

$$\frac{B'_5}{A'_1} \ln \bar{P} = \ell[\cos \phi_b - K \sin \phi_b - M] + C_1 \tag{3-98}$$

or

$$\ln \bar{P} = \frac{A'_1}{B'_5} \ell[\cos \phi_b - K \sin \phi_b - M] + C_2 \tag{3-99}$$

where C_1 and C_2 are integration constants.

The pressure at $\ell = 0$, i.e., the barrel inlet, is $P = P_1$ substituting this relation into Eqn. (3-94) gives C_2 as

$$C_2 = \ln \bar{P}_1 \tag{3-100}$$

Eqn. (3-99) now becomes:

$$\ln \frac{\bar{P}}{\bar{P}_1} = \frac{A'_1}{B'_5} \ell[\cos \phi_b - K \sin \phi_b - M] \tag{3-101}$$

Equation (3-101) indicates an exponential rise of pressure in the screw. Substituting the condition at barrel outlet, $\ell = L$, $P = P_2$, into Eqn. (3-101), gives, after rearrangement:

$$\cos \phi_b = K \sin \phi_b + M + \frac{B'_5}{A'_1 L} \ln \frac{\overline{P_2}}{\overline{P_1}} \tag{3-102}$$

Substituting the value of M (Eqn. (3-97)) into the above gives

$$\cos \phi_b = K \sin \phi_b + K\{\frac{f_s}{f_b} \frac{\overline{P_s}}{\overline{P_b}} C \sin \alpha_s +$$

$$\frac{R_b}{H} \frac{P_w}{\overline{P_b}} [\frac{1}{2} \frac{1}{f_b} (1 - C^2) + \frac{f_w}{f_b} \tan \alpha_b (1 - C)\}$$

$$+ \frac{f_s}{f_b} \frac{\overline{P_s}}{\overline{P_b}} C^2 \cos \alpha_s + \frac{f_w}{f_b} \frac{P_w}{\overline{P_b}} \frac{R_b}{H} \frac{1}{3} (1 - C^3) - \frac{1}{2} \frac{R_b}{H} \frac{P_w}{\overline{P_b}} \tan \alpha_b (1 - C^2)$$

$$+ \frac{(1 - C^2) \tan \alpha_b R_b}{2 f_b L} \ln \frac{\overline{P_2}}{\overline{P_1}}$$

This equation permits calculation of the angle of solid movement when a back pressure exists. Without a pressure difference between inlet and exit, the last term of Eqn. (3-103) drops out and it reduces to Eqn. (3-72).

CHAPTER 4

EXPERIMENTAL SET UP AND PROCEDURE

4.1 APPARATUS

Two screw feeders with different screw dimensions were used in the experiments. Feeder A (Acrison Model 105Z-H) had a metering screw with a pitch of 4 in., a screw root diameter of 7/8 in., a screw diameter of 3 in., a screw wing thickness of 3/8 in., a barrel with inner diameter of 3 1/4 in., a length of 9 in. and a 3 cubic foot hopper. A secondary 10 in. diameter ribbon type screw, of Intromitter, rotated in the hooper with the metering screw in order to give a constant supply of material to the metering screw. The screws were driven by a one horsepower D. C. motor through a reducer. The metering screw speed could be adjusted in the range of 0-100 rpm by adjusting the voltage applied to the motor. The speed ratio of the intromitter and metering screw is 1:20. Both the metering screw and discharge barrel were made of 304 stainless steel. The set up for screw feeder A is shown in Fig. 4.1.

Screw feeder B (Vibra Screw serial 175) had a screw diameter of 15/16 in., a pitch of 1 3/16 in., a screw wing thickness of 9/16 in., and no screw root. A 6 in. long, 1 in. inner diameter transparent barrel made of plexiglass was used. This permitted visual observation of the particle motion through the anger. A graduated cylinder made of plexiglass with an inner diameter of 3 5/16 in. had connected to the existing hopper which was a rectangular box with a 12 in. width and a 15 in. length. This allowed measurement of the volume of material discharged from the feeder by observing the level in the cylinder. The screw was driven by a mechanical variable speed drive.

The screw speed could be adjusted within the range 0-200rpm. To test the effect of pressure upon feed rate, the screw feeder B discharged into a columm that could be pressurized. The pressure column had a 6 inch-inner diameter and was made of plexiglass. A gas distributor was placed in the bottom of the column to support the received particles. Pressurizing air was introduced beneath the distributor. A pressure regulator was used in the air line to give a steady pressure. Two valves were used to control the pressure of the column. The first valve (right behind the pressure regulator) controlled the amount of inlet air. The second valve (on the top of the column) controlled the amount outlet air. By adjusting the two valves, the pressure in the column could be adjusted. A U-tube water monometer was used to measure the pressure. To remove particles, a plastic tube with a clamp was fitted in the lower part of the column, by fluidizing the particles and opening the clamp, the particles simply flowed out from the column through the tube. The experimental arrangement is shown in Fig. 4.2.

The material used in the experiments was sand. The particle size distribution is shown in Table 4.1.

4.2 EXPERIMENTAL PROCEDURE

The experimental procedure started with a cleaning of the screw and barrel to remove any dirt, oil or grease. Then the feeders were run with sand for 1-1 1/2 hours so that the screw and barrel surface attained an equilibrium state. Checking the feed rate at constant rpm can indicate when this has been achieved.

To measure the volumetric feed rate of screw feeder A, the weight of sand discharged from the feeder in a given time interval was recorded. The number of turns that the screw revolved during the same time period were

Table 4.1. Particle size distribution of the sand used in experiments.

Tyler Screen No.	d_p (mm)	wt%
above 14	above 1.190	.492
14 ∿ 20	1.190 ∿ .841	2.417
20 ∿ 28	.841 ∿ .595	16.651
28 ∿ 35	.595 ∿ .420	27.222
35 ∿ 48	.420 ∿ .297	35.893
48 ∿ 65	.297 ∿ .210	14.054
65 ∿ 100	.210 ∿ .148	2.400
100 ∿ 150	.148 ∿ .105	.376
150 ∿ 200	.105 ∿ .074	.145
200 ∿ 270	.074 ∿ .053	.120
below 270	below ∿ .053	.231
Summation		100%

Average diameter = $\sum_i d_{p_i} X_i$ = .45 mm

TABLE 4.2 Comparison of the Volume Change in the Hopper with the Volume Discharged from Feeder B

level change in hopper (in)	Volume Change (in^3)	Wt. Recived (gm)	Volume Calc. from Wt. (in^3)
1	8.62	230	8.7
2	17.24	445	17.0
3	25.85	680	26.0
4	34.47	910	34.7
5	43.09	1135	43.3
6	51.71	1350	51.5
7	60.33	1590	60.6
8	68.84	1800	68.6
9	77.56	--	--
10	86.18	--	--

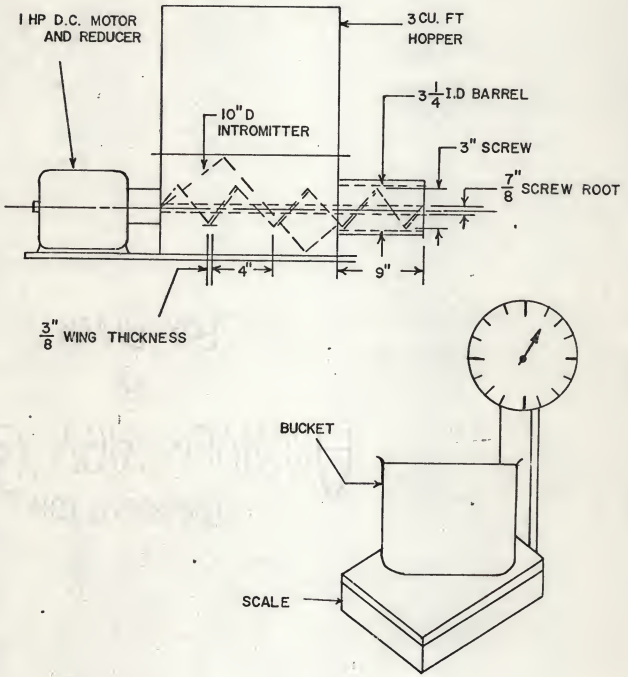

Figure 4.1. Dimensions and set up for feeder A.

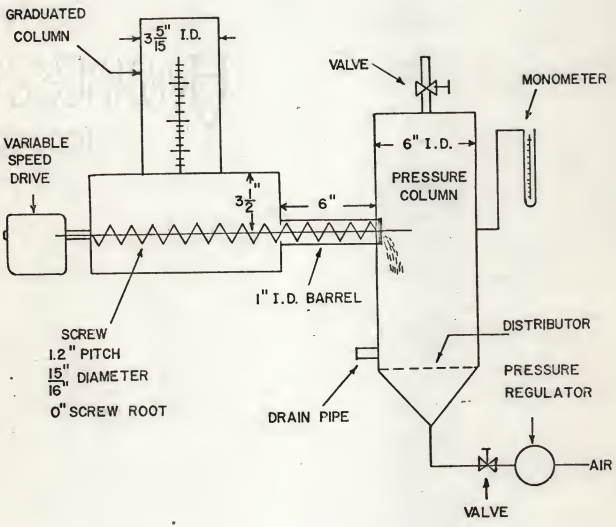

Figure 4.2. Dimensions and set up for the back pressure test on feeder B.

also recorded to determine rpm. The bulk density of sand was measured by comparing the weight of sand to the weight of water that occupied the same volume. The bulk density permitted calculation of the volumetric delivery rate. A similar procedure was used to determine the feed rate of feeder B under conditions of no back pressure.

To measure the pressure effect on the volumetric feed rate of screw feeder B, the hopper of feeder B was first filled up with sand. Then the pressure of the column was adjusted to a desired value. After selecting the desired rpm, the feeder was started. The sand level in the hopper was allowed to drop for a few inches before the recording started. This would allow the packing of sand in the hopper and the rpm to reach a steady state. Height-time data were recorded and then converted to volumetric feed rates. The actual rpm was also measured by measuring the revolutions of the screw in a given time interval. To assertain that the volume changed in the hopper can represent the actual feed rate, a calibration was conducted prior to the experiments. It followed the procedure described above, but instead the feeder discharged into a container for weighing. A comparison of the weight discharged and the volume changed in the hopper is presented to Table 4.2. As can be seen the agreement is quite good.

CHAPTER 5

CALCULATION METHOD AND TREATMENT OF DATA

5.1 CALCULATION METHOD

The volumetric delivery rate of a given screw is determined from the solid movement angle, ϕ_b, using Eqn. (3-9). In Eqn. (3-103) ϕ_b is related to the geometric variables of the screw and barrel; the friction factors f_s, f_w and f_b; the pressure difference across the barrel; the ratio between pressure at the leading wing P_w, that at the screw root, P_s, and that at the barrel surface, P_b.

$$\cos \phi_b = K \sin \phi_b + M' \tag{5-1}$$

where M' is the collection of terms on the right hand side of Eqn. (3-103) except the first term. Substituting the trigonometric relationship:

$$\sin^2 \phi_b = 1 - \cos^2 \phi_b \tag{5-2}$$

into Eqn. (4-1) yields

$$\sin \phi_b = \frac{(1 + K^2 - M'^2 - KM')^{\frac{1}{2}}}{1 - K^2} \tag{5-3}$$

For a given screw and material to be handled along with the known pressure differences between the inlet and outlet, the angle ϕ_b of Eqn. (4-3) is only a function of pressure ratios.

$$\phi_b = f\left(\frac{P_w}{P_b}, \frac{\bar{P}_s}{\bar{P}_b}\right) \tag{5-4}$$

With the assumption that $\bar{P}_s = \bar{P}_b$, ϕ_b is only a function of $P_w/\bar{P}_b$:

$$\phi_b = f'\left(\frac{P_w}{\bar{P}_b}\right) \tag{5-5}$$

From Eqn. (3-81), P_w is also a function of P* and the angle ϕ_b:

$$P_w = P^* \text{ Exp } \{-kpH \cos \bar{\alpha} \ (f_b \sin (\phi_b + \bar{\alpha}) + cf_s \sin (\alpha_s - \bar{\alpha}))/[\tfrac{1}{2}(1 - C^2) R_b]\} \quad (3\text{-}81)$$

and from Eqn. (3-83), P_b is a function of ϕ_b, P_w and P^*:

$$\bar{P}_b = \frac{1}{H \cos \alpha} \frac{2(1 - C^2) R_b P^*}{f_b \sin (\phi_b + \alpha) + Cf_s \sin (\alpha_s - \alpha)} \quad (3\text{-}83)$$

The ratio of P_w to $\bar{P}_b$ can be obtained by dividing Eqn. (3-81) by Eqn. (3-83):

$$\frac{P_w}{\bar{P}_b} = H \cos \bar{\alpha} \frac{[f_b \sin (\phi_b + \bar{\alpha}) + Cf_s \sin (\alpha_s - \bar{\alpha})]}{2(1 - C^2)}$$

$$\frac{\text{Exp } [-k_p H \cos \bar{\alpha} \ (f_b \sin (\phi_b + \bar{\alpha}) + Cf_s \sin (\alpha_s - \bar{\alpha})]}{1 - \text{Exp } [-k_p H \cos \bar{\alpha} \ (f_b \sin (\phi_b + \bar{\alpha}) + (f_s \sin (\alpha_s - \bar{\alpha})]} \quad (5\text{-}6)$$

The mean helix angle $\bar{\alpha}$ can be obtained by making use of the general equation, Eqn. (3-2):

$$\bar{\alpha} = \tan^{-1} \left(\frac{P}{\pi \bar{D}}\right) \quad (5\text{-}7)$$

where the average diameter of the screw channel will be evaluated from the weighted mean:

$$\bar{D} = 2\bar{R} = 2 \frac{\int_{R_s}^{R_b} r^2 dr}{\int_{R_s}^{R_b} r dr} = \frac{4}{3} \frac{(1 - C^3)}{(1 - C^2)} R_b = \frac{2}{3} \frac{(1 - C^3)}{(1 - C^2)} D_b \quad (5\text{-}8)$$

For a screw of known geometry (and a given material), Eqn. (5-6) is a function of ϕ_b only:

$$\frac{P_w}{\bar{P}_b} = g(\phi_b) \quad (5\text{-}9)$$

The solid movement angle at the barrel surface was evaluated by solving simultaneously Eqn. (5-9) and Eqn. (5-5). For this purpose a numerical method was used. By assuming a value of $\frac{P_w}{\bar{P}_b}$, a value of ϕ_b was found from Eqn. (5-3).

This value of ϕ_b was substituted into Eqn. (5-6) to find a new value of $\frac{P_w}{P_b}$.

This iteration was repeated until the difference between the assumed value and the generated values, D, defined as

$$D\left[\left(\frac{P_w}{P_b}\right)\text{ assumed}\right] = \left(\frac{P_w}{P_b}\right)\text{ assumed} - \left(\frac{P_w}{P_b}\right)\text{generated} \qquad (5\text{-}10)$$

became negligibly small. Specifically the combination of secant and regular falsi methods was employed. Firstly, $\frac{P_w}{P_b}$ was assumed to be zero, and then a new value of $\frac{P_w}{P_b}$ was generated and D(0) was calculated. With this new value of $\frac{P_w}{P_b}$ a second value of $D(\frac{P_w}{P_b})$ was calculated. An iteration was continued according to the scheme given in the computer flowchart in Fig. 5-1. A value of $\frac{P_w}{P_b}$ that made the absolute value of D less than a specified value was found, and eventually the value of ϕ_b was obtained from Eqn. (4-3). The delivery rate was found by substituting ϕ_b into Eqn. (3-9).

$$Q = \pi N D_b \frac{\tan \phi_b \tan \phi_b}{\tan \phi_b + \tan \phi_b} \left[\frac{\pi}{4}\left(D_b^2 - D_s^2\right) \frac{p - E}{p}\right] \qquad (3\text{-}9)$$

5.2 TREATMENT OF DATA

In the computations, the clearance between screw and barrel was neglected. The screws for both feeders were assumed to have the same diameters as the inner barrel diameters. The screw root diameter of screw feeder B was taken as 0.001 inch instead of 0. This was done to avoid the computational difficulty of evaluating the equation

$$\phi_s = \tan^{-1}\left(\frac{p}{\pi D_s}\right)$$

The sand was assumed to be isotropic, e.g., $k_p = 1$, in the computation. For the case without back pressure, the inlet pressrue and outlet pressure were equal. Since $P_2/P_1 = 1$ for this case, there was no need to evaluate

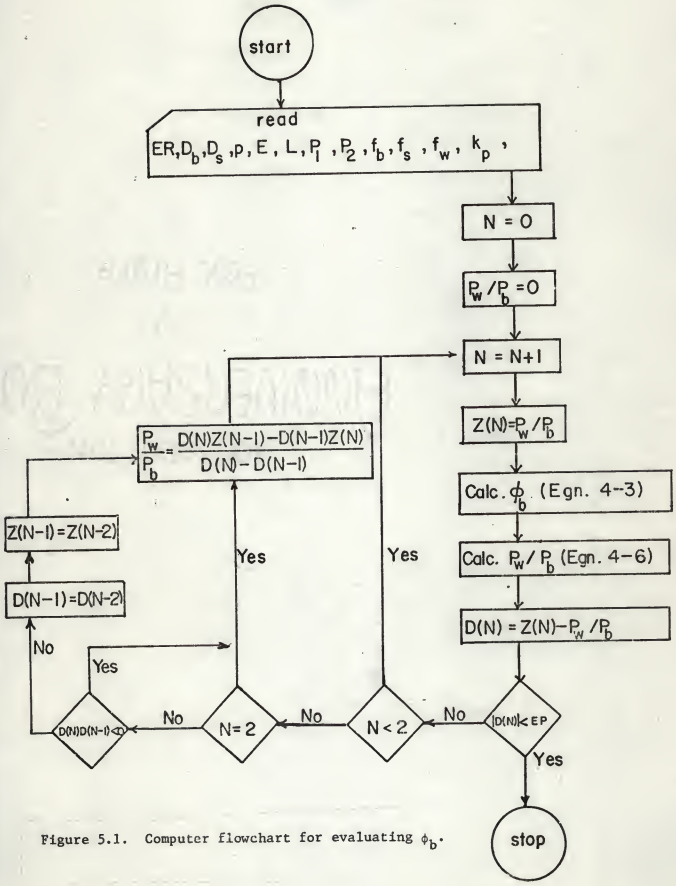

Figure 5.1. Computer flowchart for evaluating ϕ_b.

P_1 and P_2. For the cases where the back pressure exists, the pressure at the outlet of the barrel was taken as P_1 plus the back pressure, i.e.,

$$P_2 = P_1 + \Delta P$$

The back pressure ΔP was taken as the pressure difference measured from the monometer.

In the computations P_1 was assumed to be the pressure in the solid bed at the head of the screw, as it was assumed equal to the stack pressure of the solids. The static pressure of a solid stack in a container depends on the geometry of the container as well as the stack height and the density of the solids. (Ross, 1960). For a shallow bed (bed height is small compared to hydraulic radius), the pressure is proportional to the height of solid (approximately equal to the bulk density of solid times height). But with an increase in the bed height, the increase in the pressure decreases exponentially. The pressure will soon reach a final value at certain height, and adding more solids to the container has no effect on the pressure at the bottom. This phenomena can explain the constant feed rate of solids at different hopper levels before the height drops below a certain level.

For screw feeder B, this level occured about 0.5 in. from the bottom of the cylindrical hopper. This means that the sand in the cylindrical hopper had little effect on P_1. P_1 was taken as the sand bed height at the inlet of the barrel (3.5 in) times the bulk denisty of the sand.

The coefficients of friction of sand on stainless steel and plexiglass were obtained by direct measurements. Stainless and plexiglass plates under light loading were caused to slide over a bed of sand. The ratios of the forces needed to maintain the movements to the weights of the plates were taken. The coefficient of friction on stainless steel was found 0.3 and on plexiglass was 0.32.

CHAPTER 6

RESULTS AND DISCUSSION

6.1 GENERAL OBSERVATIONS ON THE EXPERIMENTS AND QUALITATIVE PRESENTATION OF DATA

During the operation of Feeder A or B, expecially at a low rpm, it became apparent that the output from the feeder was not uniform all the time, but varied periodically as the screw turns. It was not possible to measure the variation in the flow rate during each revolution of the screw with this apparatus, and consequently only a mean value taken over a period of time was obtained.

Observation through the transparent barrel of feeder B showed that all the available space between wings was occupied by sand at the inlet section of the barrel. But at the discharge end of the barrel, some void space appeared on the upper surface of the barrel. The void space increased as it approached the discharge end as shown in Fig. 6-1. At the end of the barrel, the upper part of the sand in the screw was not forced out of the barrel by the screw but appeared to flow out of the barrel by gravity. The void space in the end section decreased and the variation in output also decreased with an increase in the back pressure. The above observations suggest that the periodic output was caused in part by the effect of gravity.

The sand in the inlet section of the screw was observed to move in a helical path toward the exit. This observation supports the rigid plug assumption of the theoretical treatment. It was also observed that a portion of sand at the barrel surface (especially betwen the wing tip and barrel) moved in a somewhat random manner, particles span themself, changed directions of movement and moved in and out of the clearance of the wing tip. The

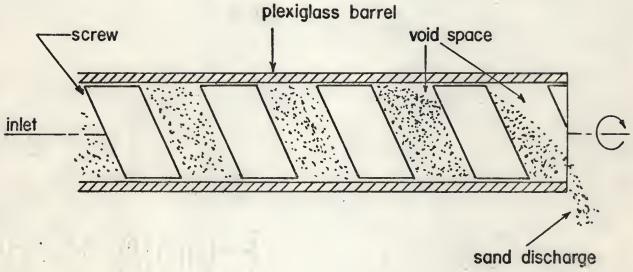

Figure 6.1. The void space at the barrel exit.

disturbance of these particles and the partial transparency caused by the abrasion of the sand, made the direct measurement of the solid movement angle difficult. The solid movement in the exit section of the barrel deviated further from the rigid plug flow pattern as a result of the creation of void space. Since the feed rate was mainly determined by the part of the screw that is running full, this phenomena should not have appreciable effects on the predicted results.

A critical hopper level was observed for each feeder, above which the feed rate at a constant rpm remained constant despite the change in the hopper level. Below this level, the feed rate at a constant rpm dropped with the level. Since the steady feed rate was of direct concern in this work, all the experiments were carried out with solid levels in the hopper above the critical level. Only a small variation in the feed rate (less than 5%) was observed in the experiments.

Figures 6.2 and 6.3 show, respectively, the mass feed rates as functions of rpm for feeder A and B. The feed rate was observed to increase linearly with an increasing rpm within the range of experiments. The volumetric delivery per revolution was almost constant at any rpm showing only a slight decline with increasing rpm. However, the feed rate at a constant rpm decreased when a back pressure was present. The larger the back pressure, the smaller the feed rate. The volumetric feed rate versus rpm at different back pressures is shown in Fig. 6.4.

6.2 COMPARISON OF THE THEORY WITH EXPERIMENTAL DATA

The theory presented in Chapter 3 is compared with experimental data in this section. Tables 6.1 and 6.2 list the exerimentally determined value of the volume delivery rate per revolution obtained with feeders A and B respectively when the back pressure is negligibly small. The

Table 6.1. Comparison of experiment and theory for feeder A

$\bar{}$rpm	screw turns	$\bar{}$total wt. (lb)	$\bar{}$wt/rev (lb)	$\bar{}$volume/rev (in^3)
4.5	20	21.94	1.10	19.0
13.7	20	21.94	1.09	18.9
20.3	20	21.60	1.08	18.7
27.2	20	21.60	1.08	18.7
38.0	$30\frac{1}{4}$	32.61	1.08	18.7
42.0	30	32.37	1.08	18.7
49.0	30	32.31	1.08	18.7
56.0	$29\frac{3}{4}$	32.04	1.08	18.7
Value predicted by the theory				18.5
Darnell and Mol's theory				15.8

Table 6.2. Comparison of experimental data with predictions for feeder B

rpm	turns	total wt. (gm)	wt/rev (gm)	volume/rev (in^3)
5	20	130.3	6.52	.249
10	40	260.1	6.50	.248
16	40	258.4	6.46	.246
22	40	256.8	6.42	.245
33	40	257.3	6.43	.245
44	60	384.3	6.41	.244
54	60	384.1	6.41	.244
81	60	383.4	6.39	.244
106	60	381.6	6.36	.243
152	60	380.0	6.33	.242
Predicted value				.245
Predicted value by Darnell and Mol's theory				.330

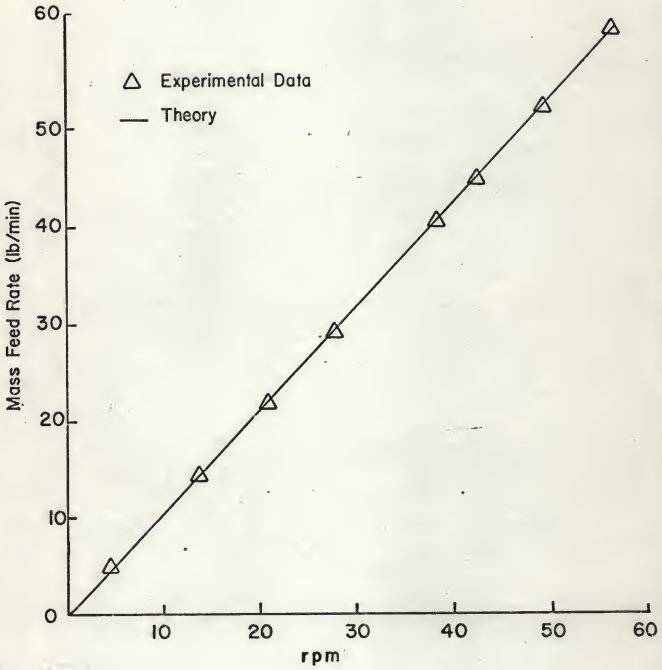

Figure 6.2. Mass feed rate versus rpm for feeder A.

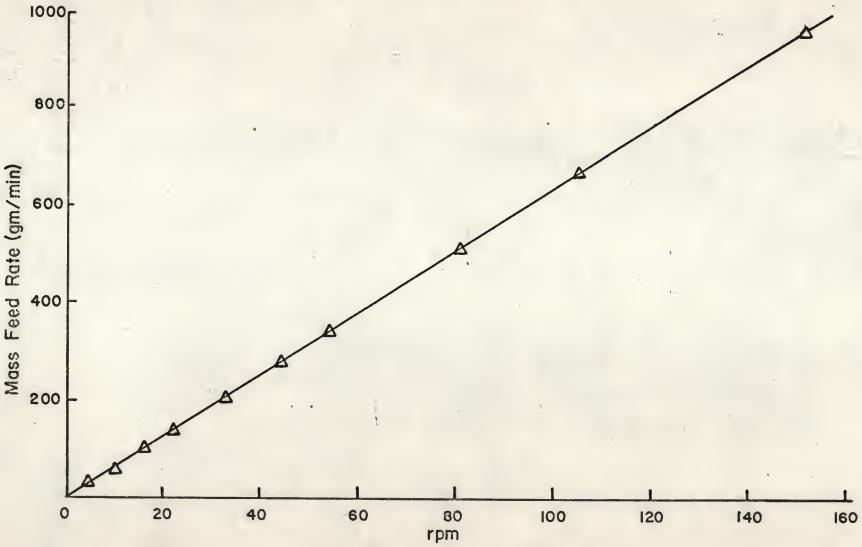

Figure 6.3. Mass feed rate versus rpm for feeder B.

theory predicts a constant volume delivery per revolution. Comparison of the predicted results from the present work and from previous theory is shown at the end of each table. It can be seen that the present theory is in good agreement with the experimental (about 3%). The prediction by Darnell and Mol's theory is too low for feeder A, but is too high for feeder B, and in each case is significantly different from the experimental results.

Figure 6.4 (in section 6.1) presents the volumetric feed rate as a function rpm for feeder B with the back pressure as the parameter. The solid lines represent the computed results based on, and the averaged experimental results (over several runs) are represented by circles for zero back pressure and triangle for a back pressure of 20 inches of water. It can be seen that the agreement is quite favorable.

Figure 6.5 shows the volume delivery rate as a function of the back pressure for feeder B operated at 54 rpm. The solid line represents the computed results based and the circles represent the experimental results. The agreement is quite good. Similar agreement was observed for the other values of rpm.

6.3 COMPARISON WITH PREVIOUS THEORY

Darnell and Mol (1956) have developed a model that is based on the solid plug concept. With the assumptions that the pressure in the solid plug is uniform, and the same coefficient of friction on the screw and barrel they used a force and torque balance to derive an equation for the solid movement angle (γ_b) for a screw with a shallow channel. Tadmor and Klein (1970) modified the treatment to include different coefficients of friction on the screw and the barrel. The resultant equation is:

Table 6.3 System parameters used by Darnell and Mol

Material	Name	Density in screw (gm/cm3)	Coefficient of friction $f_s = F_B = f_w$
1	"Zytel" 101 nylon resin	.475	.25
2	"Alathon" 10 polyethylene	.490	.40
3	"Lucite" 140 acrylic resin	.613	.50

Screw Dimensions

screw	D_b(in)	D_s(in)	$p_{(in)}$	$E_{(in)}$
C	1.991	1.375	2.00	.200
D	1.960	1.000	2.70	.125
E	1.960	1.000	2.29	.125

Table 6.4. Comparison of Darnell and Mol's experimental results with prediction values by their model and the present model.

Screw	Material	Experimental feed rate in^3/rev	Predicted feed rate (in^3/rev)		% error	
			Darnell and Mol	Present Model	Darnell and Mol	Present Model
C	1	1.91	.90	1.46	53	24
C	2	1.64	.20	1.24	88	24
C	3	1.34	.00	1.05	100	21
D	1	3.12	2.23	2.94	29	6
D	2	2.63	1.21	2.50	54	5
D	3	2.42	.30	2.11	88	13
E	1	2.83	2.25	2.80	21	1
E	2	2.88	1.50	2.51	48	13
E	3	2.88	.85	2.25	71	22

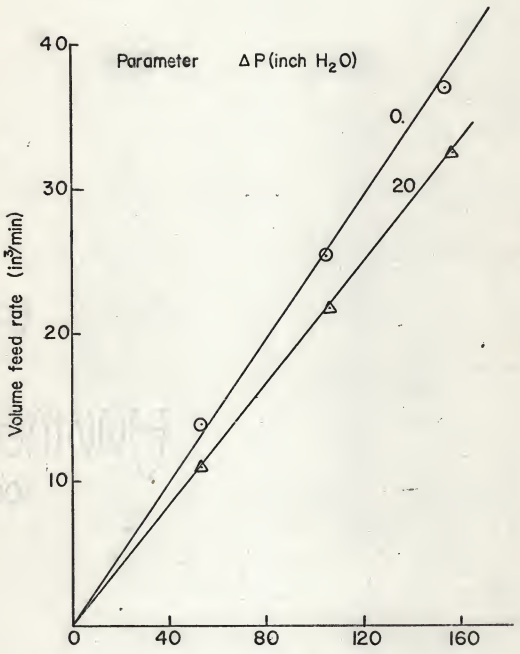

Figure 6.4. Volume feed rate of feeder B versus rpm under different back pressure conditions.

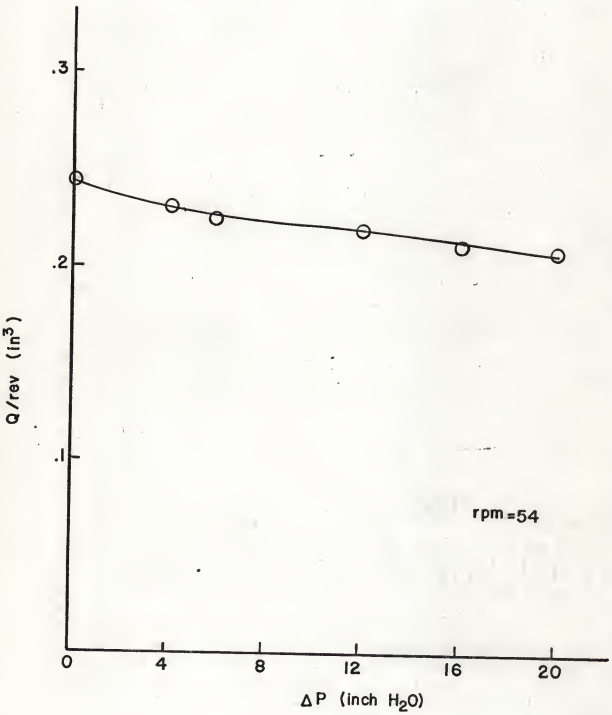

Figure 6.5. Volumtric delivery rate versus back pressure for feeder B.

$$\cos \phi_b = k \sin \phi_b + 2 \frac{(P_b - R_s)}{W_b} \frac{f_s}{f_b} \tag{6-1}$$

where

$$k = \frac{\bar{D}}{D_b} \frac{\sin \bar{\alpha} + f_s \cos \bar{\alpha}}{\cos \bar{\alpha} - f_s \sin \alpha} \tag{6-2}$$

Equation (6-1) is similar to Eqn. (3-103), but it does not contain terms in $P_w/\bar{P}_b$, and $\bar{D}$ is the arithmetic average diameter of the screw

$$\bar{D} = \frac{1}{2} (D_b + D_s) \tag{6-3}$$

The width of the channel (perpendicular to the flights) at screw tip wing can be expressed as:

$$w_b = H \cos \alpha_b \tag{6-4}$$

and at average diameter is:

$$\bar{w} = H \cos \bar{\alpha} \tag{6-5}$$

and at screw root is:

$$w_s = H \cos \alpha_s \tag{6-6}$$

and Z_b is the helical distance from inlet of the barrel following the wing tip to outlet of barrel and can be expressed as:

$$Z_b = L/\sin \alpha \tag{6-7}$$

The second term on the right hand side of Eqn. (6-1) is a result of the friction on the two wings. The third term results from the friction on the screw root and the fourth term is from the back pressure. An additional force on the wing is needed to balance the other force and is given by

$$F^* = \frac{dZ_b \left(f_b w_b \sin\phi + 2(R_b - R_s) f_s \sin \alpha_s + w_s f_s \sin \alpha_b P\right)}{\cos \bar{\alpha} - f_s \sin \bar{\alpha}} + H \bar{w} \sin \bar{\alpha} dP \tag{6-8}$$

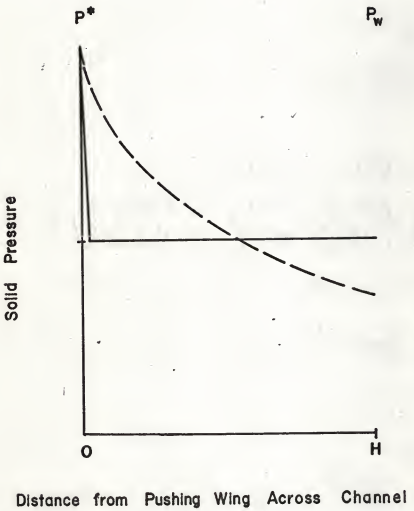

Figure 6.6. Pressure distribution in the cross channel direction.

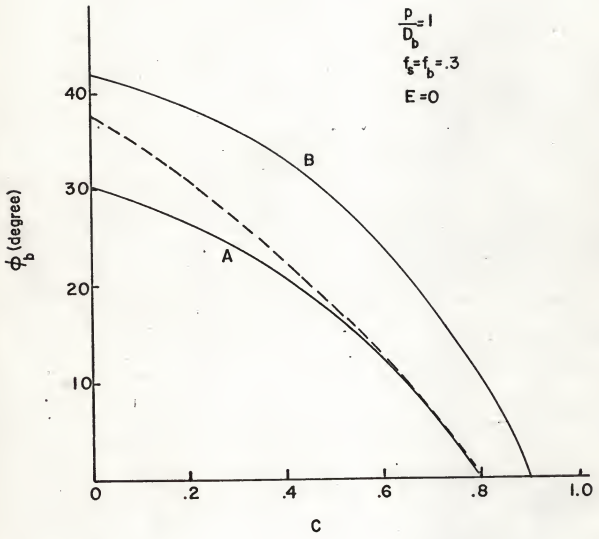

Figure 6.7. Comparison the present work with Darnell and Mol's theory.

and it acts in a direction normal to the wing surface at $\bar{R}$. The pressure distribution in a solid plug contained between the two wings is assumed to be:

$$P = P^* = P_w + P_A \text{ for } h = 0 \tag{6-9}$$

$$P = P_W = \bar{P}_b \text{ for } 0 < h \leq H \tag{6-10}$$

where P_A is the additional pressure caused by P*.

From calculation, the value for P_A is about 1 to 2 time of the value of P_W. Figure 6.6 shows a plot of the pressure distribution in the cross channel direction for a solid element. The dotted line represents the solid pressure distribution in cross channel direction considered in the present thesis. The solid line represents the pressure distribution considered in Darnell and Mol's theory.

Figure 6.7 presents a comparison of Eqn. (3-103) and Eqn. (6-1), and, in terms of a plot of ϕ_b versus C, calculations were made for the following conditions: $p = D_b = 1$, $f_s = f_b = 0.3$ and $E = 0$. Line A results from Eqn. (3-103) with P_w/P_b equal to 1, or uniform pressure distribution. Line B represents the case where the nonuniform distribution was considered. From the figure, it can be seen that without considering the pressure distribution in the solid plug, Eqn. (6-1) which is represented by the dotted line agrees with Eqn. (3-103) when the channel is shallow (C close to 1), but deviates significantly when the channel is deep. With the consideration of nonuniform pressure distribution in the solid plug, a higher value of ϕ_b was predicted.

Darnell and Mol (1956) also published some experimental data on the volumetric feed rates in screw feeders. Three different screw sizes and three different materials were used in their experiments. The system parameters are shown in Table 6.3. When theoretical volumetric feed rate

per revolution of Darnell and Mol are compared to the theoretical values using the model developed in this thesis in Table 6.4, it is seen that the present model provides a significant improvement in the description of the data.

6.4 SIMULATION STUDIES

The feed rate of a screw is expressed by Eqn. 3-9 in terms of the screw geometry, the solid movement angle, and the speed of revolution;

$$Q = \pi N D_b \frac{\tan \phi_b \tan \alpha_b}{\tan \phi_b + \tan \alpha_b} \left[\frac{\pi}{4} (D_s^2 - D_s^2) \frac{p - E}{p}\right] \tag{3-9}$$

In order to discuss and compare the efficiency of a screw's output, the volumetric efficiency is defined as the ratio of the actual feed rate to the sweep volume of the screw. The sweep volume of a screw can be expressed as:

$$V_s = Np \left[\frac{\pi}{4} (R_b^2 - R_s^2) \frac{p - E}{p}\right] \tag{6-11}$$

Substituting for p (the pitch) from Eqn. (3-1) outside the brackets in Eqn. (6-11) permits the volumetric efficiency of a screw to be expressed as:

$$\eta = \frac{Q}{V_s} = \frac{\tan \phi_b}{\tan \phi_b + \tan \alpha_b} \tag{6-12}$$

From Eqn. 6-12, the volumetric efficiency is only a function of the solid movement angle and the helix angle at the barrel surface. The helix angle at the barrel surface can be expressed in terms of the ratio of the pitch to screw diameter from Eqn. 3-1.

$$\tan \alpha_b = \frac{p}{\pi D_b} \tag{3-1}$$

Figure 6-8 presents the volumetric efficiency as a function of the solid movement angle for different ratios of pitch to screw diameter. It can be seen that for a fixed helix angle, the larger the solid movement angle, the larger the volumetric feed rate.

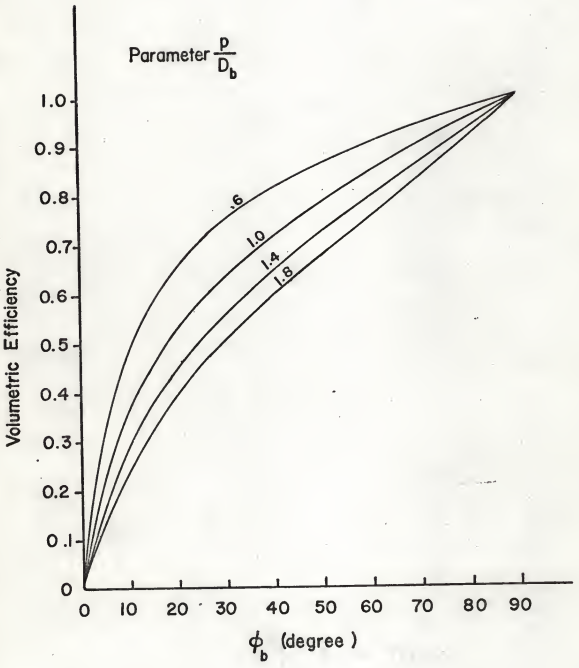

Figure 6.8. Volumetric efficiency versus solid movement angle.

By expressing the helix angle in terms of p and D_b, Eqn. (3-103) can be put in an alternate form:

$$\cos \phi_b = K \sin \phi_b + K\{\frac{f_s \bar{P}_b}{f_b \bar{P}_b} C \frac{(p/D_b)}{(\pi C^2 + (p/D_b)^2)^{\frac{1}{2}}} + \frac{1}{2(1 - \frac{E}{D_b})}$$

$$\frac{P_w}{P_b} [\frac{1}{2} \frac{1}{f_b} (1 - C^2) + \frac{f_w}{f_b} \frac{p}{\pi D_b} (1 - C)]\} + \frac{f_s}{f_b} \frac{\bar{P}_s}{\bar{P}_b} C^2$$

$$\frac{\pi C}{(\pi C^2 + (\frac{p}{D_b})^2)^{\frac{1}{2}}} + \frac{f_w}{f_b} \frac{P_w}{\bar{P}_b} \frac{1}{2(1 - E/D_b)} \frac{1}{3} (1 - C^3) - \frac{1}{4}$$

$$\frac{1}{(1 - E/D_b)} \frac{P_w}{\bar{P}_b} \frac{1}{\pi} (\frac{p}{D_b}) (1 - C^2) + \frac{(1 - C^2)}{2} \frac{1}{2(p/D_b)}$$

$$\frac{1}{\pi} (\frac{p}{D_b}) \quad (\frac{p}{D_b}) \ln \frac{\bar{P}_2}{\bar{P}_1} \tag{6-13}$$

This equation is a dimensionless equation in terms of the following dimensionless variables: coefficients of friction; f_s, f_b, and f_w, ratios of pressures; $P_w/\bar{P}_b$, and P_1/P_2; and screw geometry, P/D_b, E/D_b, and L/D_b. The model assumes $\bar{P}_s/\bar{P}_b = 1$, and $P_w/\bar{P}_b$ can be related to other parameters as discussed in section 3.4, and f_s is usually equal to f_w. Thus, ϕ_b can be expressed as

$$\phi_b = G(\frac{p}{D_b}, C, \frac{E}{D_b}, \frac{L}{D_b}, f_s, f_b, \frac{\bar{P}_1}{\bar{P}_2}) \tag{6-14}$$

The effects of the variables in the right hand side of Eqn. (6-14) will be numerically based on the present model, for the case of, $f_s = f_b$, and no back pressure, $P_1 = P_2$. The effects of screw geometry are considered first. Figure 6-9 shows the effect of the dimensionless screw root diameter or C on ϕ_b. For a square pitch $P = D_b$ and and an idealized screw ($E = 0$). It

can be seen that as the screw root diameter increases, ϕ_b decreases and ϕ_b eventually goes to zero as C approaches to 1. Further, the smaller the coefficient of friction, the larger the ϕ_b.

In Fig. 6-10, the effect of wing thickenss on ϕ_b is presented when $p/D_b = 1$ and $C = 0.5$. The figure shows that the larger the wing thickness, the smaller ϕ_b. It can also be seen that ϕ_b will go to 0, if the wing is too thick. At a fixed E/D_b, ϕ_b also decreases as f increases.

Figure 6-11 illustrates the effect of pitch on ϕ_b computation when $C = 0.5$, and $E = 0$. It can be seen that for a too small pitch, ϕ_b will be zero first, then raise rapidly to a maximum then begin to decline. It will go to zero again if p/D_b is large enough. At fixed p/D_b, ϕ_b decreases as f increases. The location of the maximum ϕ_b varies slightly with the coefficient of friction and lies in the range of $0.7 < p/D_b < 1.2$. This agrees with the fact that most screws used in industry have a pitch to screw diameter of about 1.

From Eqn. 6-11, it can be seen that the length of the barrel has no effect on ϕ_b when there is no back pressure. This prediction is confirmed by the observation of Roberts and Willis (1962) and many other investigators of screw conveyors, since the length of the barrel has never been listed as a factor effecting the output of a screw conveyor.

The effect of different coefficients of friction on ϕ_b is shown in Fig. 6-12. The simulation was based upon a $p/D_b = 1$, $E = 0$, and $C = 0.5$. The figure presents a plot of ϕ_b versus f_b/f_s value, the larger the ϕ_b. At fixed f_b/f_s, the smaller the f_s, the larger the ϕ_b. This behavior is apparently well-known as it has been suggested that the screw be coated with Teflon and that the barrel be roughened up (Cann.).

Next, the effects of back pressure are examined numerically for the case of $p/D_b = 1$, $C = 0.5$, $E = .5$. Figure 6-13 presents a plot of ϕ_b versus

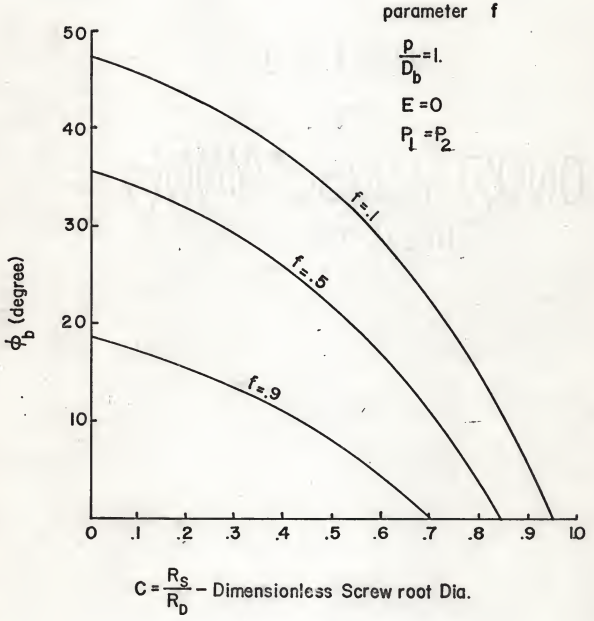

Figure 6.9. Effect of screw root diameter on ϕ_b.

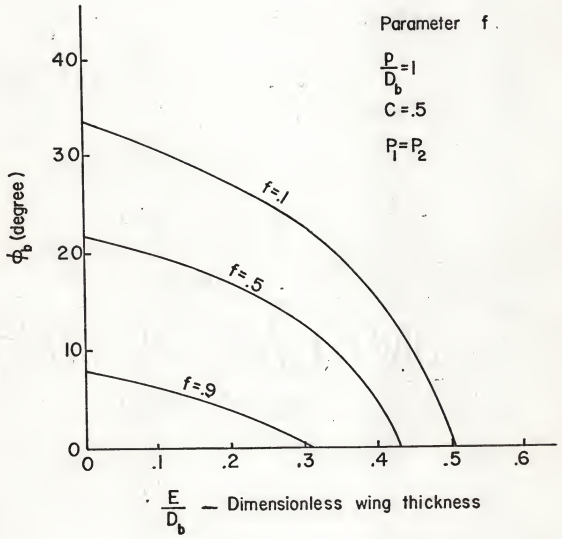

Figure 6.10. Effect of wing thickness on ϕ_b.

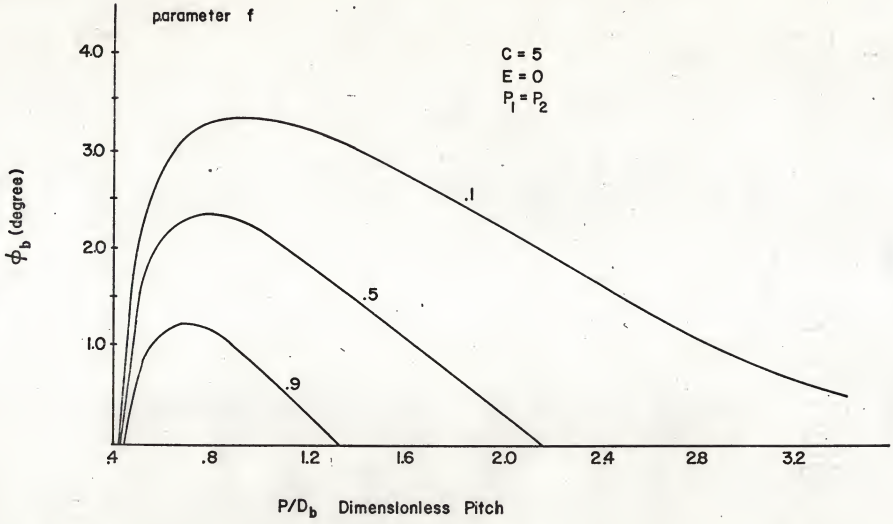

Figure 6.11. Effect of pitch on ϕ_b.

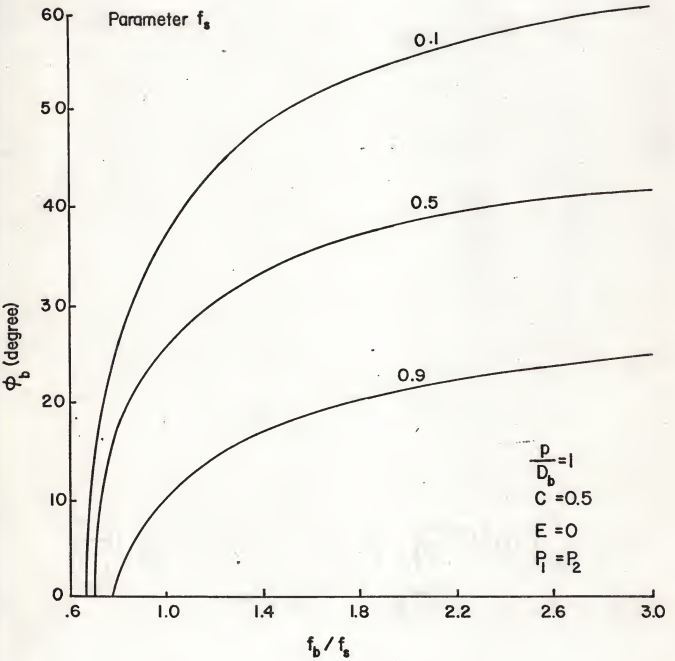

Figure 6.12. Effect of friction ratio on ϕ_b.

$(\ln P_2/P_1)/(L/D_b)$. The smaller the coefficient of friction, the more rapidly ϕ_b decreases, or the greater the influence of back pressure. It can also be seen that ϕ_b is reduced when the ratio

$$(\ln \frac{P_2}{P_1})/L/D_b$$

becomes sufficiently large.

Figure 6-14 plots ϕ_b against P_2/P_1 for the conditions of Fig. 6.13 with barrel length as the parameter when f = .3. The figure shows that the influence of back pressure diminishes with increasing barrel length.

The effects of C and E on ϕ_b when back pressure existed are shown in Figure 6-15 and 6-16 respectively. Figure 6-15 plots ϕ_b against P_2/P_1 with C as the parameter for the case of $p/D_b = 1$, $L/D_b = 5$, f = 0.3, E = 0. At a fixed P_2/P_1 ratio, it can be observed that the smaller the C, the larger the ϕ_b.

Figure 6-16 plots ϕ_b against P_2/P_1 with E as the parameter. The conditions of simulation were $p/P_b = 1$, $L/D_b = 5$, f = .3, C = .5. At a fixed P_2/P_1 ratio, the smaller the E, the larger the ϕ_b.

The above results suggest that, in designing a screw feeder, for an operation with or without back pressure, a small screw root diameter and a small wing thickness are necessary and desirable to achieve a high feed rate. For an operation with a back pressure, the longer the barrel, the smaller the influence of back pressure and the higher the limit of back pressure. But, since the strength of the screw will decrease as the screw root diameter and wing thickness decrease, some trade-offs will have to be made. Further, the longer the barrel, the more power it will consume; again, trade-offs will have to be made. The optimum design for the geometry of a screw should be determined by the operating conditions of the application.

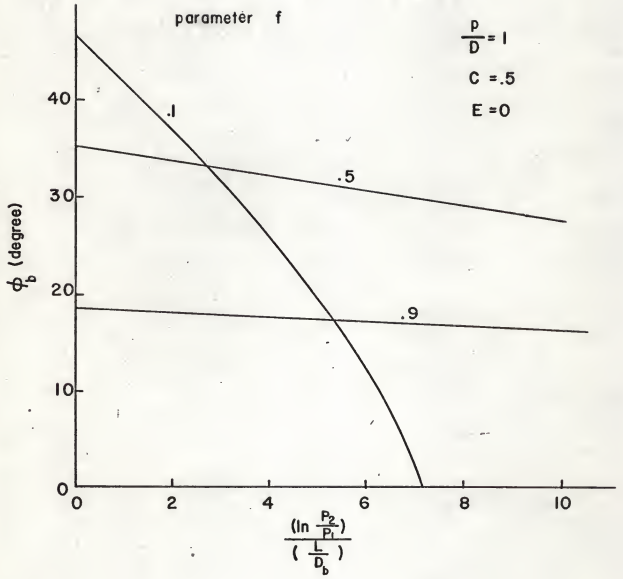

Figure 6.13. Effect of $(\ln P_2/P_1)/L/D_b$ on ϕ_b.

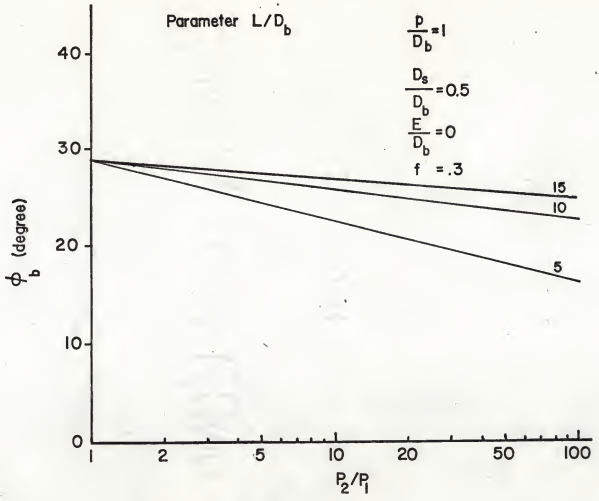

Figure 6.14. Effect of P_2/P_1 on ϕ_b under different L/D_b.

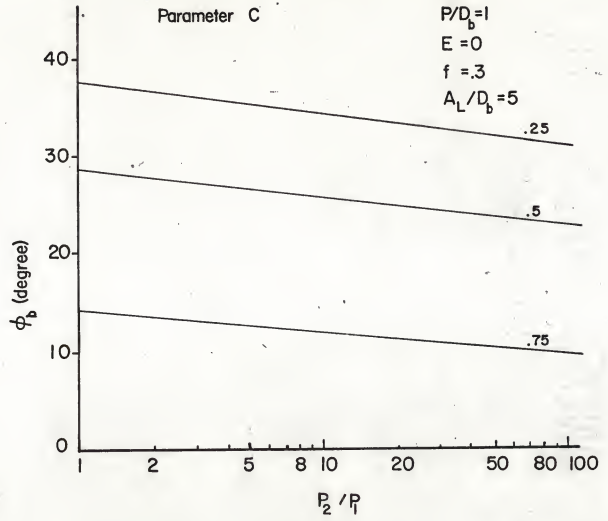

Figure 6.15. Effect of P_2/P_1 on ϕ_b under different C.

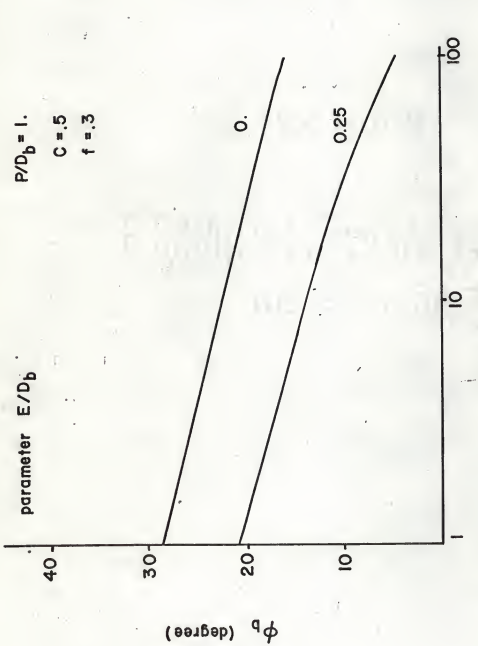

Figure 6.16. Effect of P_2/P_1 on ϕ_b under different E/D_b.

CHAPTER 7

CONCLUDING REMARKS AND SUGGESTIONS FOR FUTURE WORK

The mechanism of solid transport in a screw feeder is still uncertain despite of its wide use in industry. The difficulties in describing the mechanism arise from the complexity of describing both the particle movement and the curvature of the screw. In this work, equations have been formulated to predict the volumetric feed rate of a screw feeder working in a horizontal position. It was assumed that all the particles conveyed in the screw feeder move as a rigid plug at a constant speed. It is possible, with this assumption, to develop a model for estimating the solid movement angle. The feed rate of the screw feeder can then be readily obtained from this angle. To simplify the treatment, some additional assumptions were introduced. These include negligible clearance and constant coefficients of friction. A force balance on a solid plug enables one to express the solid movement angle at the barrel surface in terms of screw geometry, coefficients of friction, pressure rise and the ratio of the solid pressure on the leading wing to the average pressure on the barrel surface. A simplified model which neglects the curvature of the wing was used to obtain the pressure distribution in the solid plug. This information is necessary to calculate the solid movement angle.

Comparisons were made between experimentally determined and predicted values of the feed rates for two screw feeders conveying sand for selected speeds from zero to 200 rpm. The deviation between the experimental and predicted values of the volumetric feed rate was less than three percent.

The model used in this study considered two important variables that previous workers had neglected. These variables are the pressure distribution in the solid plug and the change of screw angle with the diameter of the screw. Due to the inclusion of these features, the improvement in the model is significant. For example, the average deviation between the experimental data and the theoretical values based on the model of Darnell and Mol 61%; in contrast, the average deviation between the experimental data and the theoretical values based on the present model was 14%.

Significant time saving can probably be made in the design of screw feeder or a conveyor using this model. Previously, feeders were designed by trial and error and from data of similar feeders. In addition, the effect of changes in operating conditions on the feed rate was uncertain. By using the model developed in this thesis, it is hoped that a feeder can be quickly and accurately designed and optimized with a minimum of trial and error.

The controversial assumptions made in the screw feeder model were that the solids always moved in plug flow and that the solid pressure against the screw wing is uniform irrespective of the radius. Although the plug flow assumption is quite realistic for most cases, it will not accurately describe the solid movement under some conditions. These conditions are as follows. If the screw is not full of solids, or the clearance between the screw and barrel is large, or the internal friction among particles is smaller than that between the barrel and screw, the plug flow assumption is not applicable. The uniform pressure assumption has not been examined, either experimentally or theoretically. Consequently, more research should be done on developing a model that can account for flows other than plug flow and variable pressure over the channel depth.

The centrifugal and gravitational forces are also not considered in the present model. Therefore, the results of this work are applicable only to horizontal feeders operating at low rpms. Inclusion of gravitational and centrifugal forces in the analysis will expand the versatility of the present model to inclined screw feeders and conveyors, and permit considerations of high operational speeds.

LITERATURE CITED

Anakin, I. A., "An Analysis of the Work of Combine Augers," Selkhozmashina, No. 5 (1953).

Broyer, E., and Tadmor, Z., "Solids Conveying in Screw Extruders, Part I: A Modified Isothermal Model," Polym. Eng. Sci., 12, 12 (1972).

Cann, J. R., British Patent 715, 920.

Darnell, W. H., and Mol, E.A.J., "Solids Conveying in Extruders," Soc. Plastics Eng. J. 12, 20 (1956).

Decker, H., "Die Spritzmachine," Paul Troester Maschinenfabrik, Hanover, Germany (1941).

Jackson, M. L., Lavacot, F. J., and Richards, H. R., "The Extrusion Theory with Application to Double Base Propellent," Ind. Eng. Chem., 50, No. 10, 1569 (1958).

K. Önig, A., and Riemann U., "Untersuchungen am senkrechten Schneckenförderer," Landtch. Forsch., Münch., 10, No. 2, 45 (1960).

Lovegrove, J.G.A., "Solid Flow in a Polymer Extruder," Ph.D. Thesis, University of London (1972).

Lovegrove, J.G.A., and Williams, J. G., "Solids Conveying in a Single Screw Extruder - The Role of Gravity Force," J. Mech. Eng. Sci., 15, No. 3, 114 (1973a).

Lovegrove, J.G.A., and Williams, J. G., "Solids Conveying in a Single Screw Extruder, A Comparison of Theory and Experiment," J. Mech. Eng. Sci., 15, No. 3, 195 (1973b).

Lovegrove, J.G.A., and Williams, J. G., "An Examination of Stress in Solid Being Conveying in a Single-Screw Extruder," J. Mech. Eng. Sci., 16, No. 5, 281 (1974).

Maillefer, C., Doctoral Thesis, University of Lausanne (1952).

Metcalf, J. R., "The Mechanics of the Screw Feeder," Proc. Instn. Mech. Eng., 180, No. 6, 131 (1965-66).

Millier, W. F., "Bucket Elevators, Augers Conveyors for Handling Free Flowing Materials," Agric. Eng. 39, No. 9, 552 (1958).

Mistry, D. K., "Development of a Continuous Dry Coal Screw Feeder, PHASE 11," ERDA Report FE-1744-16 (1976).

Mistry, D. K., "Development of a Continuous Dry Coal Screw Feeder, PHASE II," ERDA Report, FE-1794-19 (1977).

Morin, I. V., "Auger Output," Nat. Inst. Agri. Eng. Trans. 77, Silsoe (1956).

O'Callaghan, J. R., "Performance of Vertical Screw Conveyors," Agric. Eng. 40, No. 8, 450 (1959).

Pawlowski, J., unpublished report, Dormagen, Farbenfabliken Bayer, Germany (1949).

Peart, M., "Vertical Augers for a Silo Unloader," University of Illinois Bulletin, No. 631 (1958).

Regan, W. M., and Henderson, S. M., "Performance Characteristics of Inclined Screw Conveyors," Agric. Eng. 40, No. 8, 450 (1959).

Rehkugler, G. E., "Performance of Auger Conveyors for Handling Grains and Ground Feeds," Agri. Eng. Extension Bulletin 325 (1959a).

Rehkugler, G. E., "Performance Characteristics of Farm Type Auger Elevator," Paper presented at North Atlantic section Amer. Soc. Agric. Eng., September 1-3 (1959).

Roberts, A. W., and Willis, A. H., "Performance of Grain Augers," Proc. Instn. Mech. Eng., 176, No. 8, 165 (1962).

Ross, I. J., "The Force Acting on Particles Stacks and Capacity of Enclosed Screw Conveyors," Master Thesis, Purdue University (1960).

Schneider, K., "Technical Report on Plastics Processing - Processes in the Feeding Zone of an Extruder," Kunststoffe, 59, 97 (1969).

Simonds, H. R., Weith, A. J., and Schack, W., "Extrusion of Plastics Rubber and Metals," Reinhold Publishing Corp., New York (1952).

Stevens, G. N., "Performance Test on Experimental Auger Conveyors," J. of Agric. Research, 7, No. 1, 47 (1962).

Tadmore, Z., and Klein, I., "Engineering Principles of Plasticating Extrusion," Chapter 4, Van Nostrand Reinhold Co., New York (1970).

Weber, F., Technik, 2, 456 (1947).

Wright, D. C., American Machinist, 64, No. 24 (1926a).

Wright, D. C., American Machinist, 65, No. 1 (1926b).

Zaika, P. M., "Ovybooe Barametrov Vintovykn Transporterov Zernovykh Kombainov," Trakt i Selkn Mash., 1, 22 (1958).

Zimmer, G. F., "The Mechanical Handling of Materials," Van Nostrand, New York (1905).

Zimmer, G. F., "The Mechanical Handling and Storing of Material," The London Technical Press, London (1932).

TRANSPORT OF SOLIDS IN A SCREW FEEDER

by

CHERNG-CHIAO WU

B.S., National Taiwan University, 1973

AN ABSTRACT OF A MASTER'S THESIS

submitted in partial fulfillment of the

requirements for the degree

MASTER OF SCIENCE

Department of Chemical Engineering

KANSAS STATE UNIVERSITY

Manhattan, Kansas

1977

ABSTRACT

Screw feeders and screw conveyors have been widely used in industry and in farming operations as particle handling devices. However, theoretical approaches to describe the performance of screw feeders and enclosed screw conveyors are at present unsatisfactory. The purpose of this study was to develop a suitable theoretical approach for describing the performance of screw feeders.

The device considered here is a screw rotating in a tightly fitted barrel, and the particles fill up all the available space in the screw channel. It was assumed that all the particles conveyed in the screw move like a rigid plug at constant velocity. Then the delivery rate of the device could be related to the r.p.m. of the screw, geometry of the screw, and the direction of the solid plug movement. With the aid of a force and work balances on a small section of the solid plug and an analysis of the solid pressure distribution in the plug, the angle of solid movement was expressed in terms of screw geometry, coefficients of friction of the particles on the screw and barrel surfaces, and the pressure exerted on the inlet and outlet of the screw feeder. With the angle of solid movement established, the delivery rate can be evaluated directly.

Two screw feeders with screw diameters of 15/16" and 3 1/4" respectively, were used in the experiments. Comparisons were made between the experimentally determined and predicted values of the delivery rate for both feeders operating under conditions of no back pressure up to 20" of water. The difference between the experimentally determined and predicted delivery rates were found to be no more than ten percent of the experimentally measured values.